Award Number: W81XWH-12-1-0476

TITLE: 'An Injectable Method for Posterior Lateral Spine Fusion

PRINCIPAL INVESTIGATOR: Dr. Jennifer West

CONTRACTING ORGANIZATION: Duke University
Durham, NC 27708

REPORT DATE: September 2015

TYPE OF REPORT: Annual

PREPARED FOR: U.S. Army Medical Research and Materiel Command
Fort Detrick, Maryland 21702-5012

DISTRIBUTION STATEMENT: Approved for public release; distribution unlimited

REPORT DOCUMENTATION PAGE

Form Approved
OMB No. 0704-0188

1. REPORT DATE *(DD-MM-YYYY)*	2. REPORT TYPE	3. DATES COVERED *(From - To)*
September 2015	Annual	1SEP2014 - 31AUG2015

4. TITLE AND SUBTITLE

'An Injectable Method for Posterior Lateral Spine Fusion

5a. CONTRACT NUMBER

5b. GRANT NUMBER
W81XWH-12-1-0476

5c. PROGRAM ELEMENT NUMBER

6. AUTHOR(S)
Dr. Jennifer West; Dr. Elizabeth Olmsted-Davis; Dr. Alan R. Davis,;and Dr. Eva Sevick- Muraca

email: jennifer.l.west@duke.edu

5d. PROJECT NUMBER

5e. TASK NUMBER

5f. WORK UNIT NUMBER

7. PERFORMING ORGANIZATION NAME(S) AND ADDRESS(ES)
Duke University
Durham, NC 27708

8. PERFORMING ORGANIZATION REPORT NUMBER

9. SPONSORING / MONITORING AGENCY NAME(S) AND ADDRESS(ES)
U.S. Army Medical Research And Materiel Command
Fort Detrick, Maryland 21702-5012

10. SPONSOR/MONITOR'S ACRONYM(S)

11. SPONSOR/MONITOR'S REPORT NUMBER(S)

12. DISTRIBUTION / AVAILABILITY STATEMENT

Approved for Public Release; Distribution Unlimited

13. SUPPLEMENTARY NOTES

14. ABSTRACT: The central hypothesis of this application is that posterolateral spine fusion can be successfully achieved with a novel and simple minimally invasive percutaneous injection. We propose that this can be done by injection of AdBMP2 transduced human fibroblasts possessing an icasp9M that have been micro-encapsulated with osteoclast degradable hydrogel into the desired fusion site. During the course of this grant application we observed that in the rat model, we were unable to induce the heterotopic bone formation necessary to fuse the spine. Since this is a major stumbling block for the development of this therapy, we compared the process in mice to rats and found that MMP9 activation was not active, but rather existed as in the proform. This is very different from mice or even humans where all MMP9 at the site of HO is active. Additionally, we confirmed that the lack of bone formation after delivery of the microspheres to larger animal models was not the result of an immune response to the adenovirus transduced cells encapsulated in the PEG-Da hydrogels. The results showed that mice previously exposed to adenovirus transduced cells totally suppressed the bone formation ability of the AdBMP2 transduced cells, however, if they were encapsulated in the PEG-Da hydrogel, then bone formation proceeded as expected. Thus the hydrogel can overcome cellular immunity associated with the materials. Finally, we have shown that we can attentuate the bone formation through inclusion of a stably integrated icasp9M that leads to rapid apoptosis in the hydrogel encapsulated cells *in vivo*, after exposure to a chemical inducer of dimerization (CID). The work is the focus of 4 manuscripts.

15. SUBJECT TERMS
BMP2, Spine fusion, PEG hydrogel, Gene Therapy, Adenovirus

16. SECURITY CLASSIFICATION OF:			17. LIMITATION OF ABSTRACT	18. NUMBER OF PAGES	19a. NAME OF RESPONSIBLE PERSON
a. REPORT	b. ABSTRACT	c. THIS PAGE			USAMRMC
U	U	U	UU	51	19b. TELEPHONE NUMBER *(include area code)*

Table of Contents

Page

1. INTRODUCTION: The treatment of many spinal problems involves stabilization of the spine by applying bone grafts to the posterior elements of the spine. The objective of these procedures is to induce bone to bridge between adjacent vertebral bodies and "fuse" the vertebrae into a larger bone mass. Posterolateral fusion of the spine is the most commonly performed of all the types of spine fusion and is useful for the treatment of scoliosis, instability and painful degenerative conditions of the spine. We recently demonstrated that adenovirus transduced cells expressing BMP2, when injected into the paraspinous musculature, could rapidly form new bone at the targeted location and efficiently fuse vertebral bone at a desired site, within 2 weeks. Encapsulation of these cells in poly(ethylene glycol)-diacrylate (PEGDA) hydrogels allowed for longer survival of the cells *in vivo*, did not result in inflammation, which otherwise completely ablate new bone formation/fusion, and maintained the cells at the target location. Thus our preliminary data demonstrates the ability to induce new bone formation at the desired fusion location without need for any surgical intervention. Here we propose to engineer additional safety features into the material by using an inducible caspase 9 ($icasp9_M$), which when activated will induce apoptosis within the transduced cells. Further, the hydrogel will also possess an osteoclast selective protease site which allows for removal of the biomaterial during bone remodeling.

2. KEY WORDS: BMP2, Spine Fusion, PEG hydrogel, Gene therapy, Adenovirus

3. ACCOMPLISHMENTS: ***The major goals for each aim are listed along with the accomplishments?***

Task 1: To characterize the ability of the molecular therapy system to rapidly induce fusion of the new bone with the vertebra, through induction of osteoclast progenitors (OCP) – monocyte progenitors. The proposed studies in this aim are an extension from our previous findings that monocyte-like cells that are not multinucleated osteoclasts were observed at the fusion site between the new heterotopic

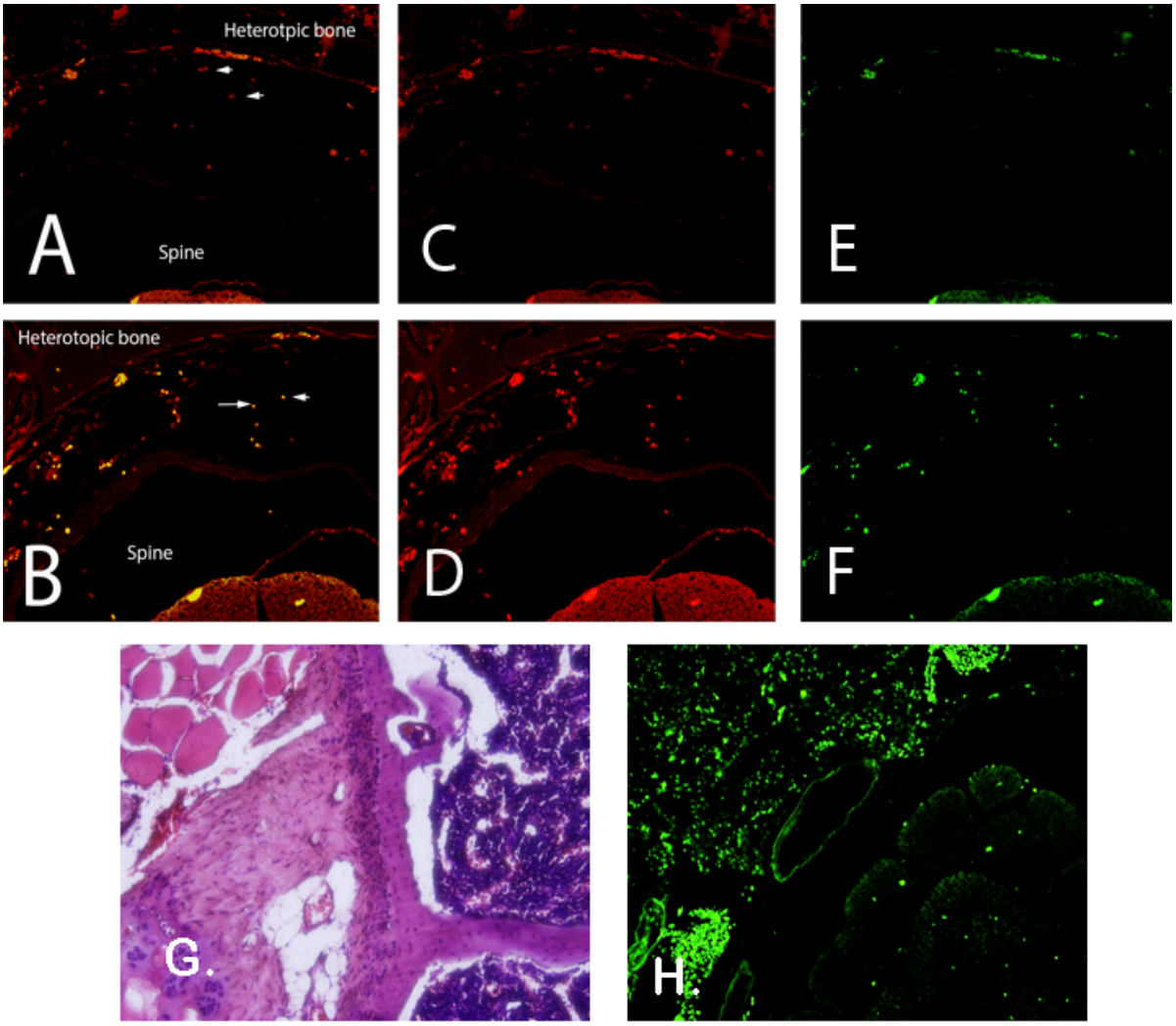

Figure 1: Representative photomicrographs of tentative vertebral fusion with the heterotopic bone. The slides were immunostained for **(A and C)** CD11b (red), **(A and E)** fractalkine (green) and merged in **(A)**. In panels **(B and D)** fractalkine (red), **(B and E)** LyC6 (green), and **(G)** hematoxylin and eosin for viewing. Panel H depicts a nerve with positive staining for LyC6 in the perineurium. These are representative photomicrograph (10X) of a sample taken 4 weeks after the initial injection of AdBMP2 transduced cells.

bone, and skeletal bone (figure 1). These cells appeared to be contributing to the remodeling of the fusion structure, and may be critical to enhancing fusion between the two bones. We propose that if we could characterize and isolate these cells, they may be beneficial in enhancing spine fusion, in other model systems as well as our own. One of the first steps is to determine their phenotype and determine if they are actually specialized M2 macrophages expanded to aid in matrix remodeling and fusion.

Therefore we have secured animal approval for the studies, and performed spine fusion in mice to generate tissue sections for initial phenotypic characterization of these spines. In these experiments, mice (n= 4) were injected with AdBMP2 or Adempty transduced cells and then spines isolated at weekly intervals (1-6 weeks) and serial sections generated, that represent the fusion process in the animals. We then initiated immunohistochemical staining with key antibodies that will be used for fluorescence activated cell sorting (FACs). These antibodies (CD11b ^{lo}, fractalkine^{+}, Ly6C^{+}), are surface antigens that can readily allow us to sort populations of cells for testing in bone resorption assays. After initial optimization of the antibodies, we observed co-localization of fractalkine^{+} and Ly6C^{+} in the cells, but as expected they were not expressing CD11b (figure 1). These cells were found lining the junction between the heterotopic bone and the new bone (figure 1, panel B). What was further intriguing was that cells associated with the perineurium of the nerve were also LyC6^{+} but not fractalkine^{+}. It is unclear whether these cells may function as an earlier progenitor, or whether they are just a separate population. We will continue to characterize this phenotype.

The next step is to isolate and further characterize the phenotype of these cells specifically to demonstrate their potential M2 nature. Also we will collect the various positive and negative populations and confirm their bone resorption ability using a standard assay kit (Bone Resorption Assay Kit; CosmoBio Co, Ltd) that uses a fluoresceinated calcium phosphate-coated plate. Additionally, we will isolate and test these cells *in vitro* to determine whether they respond to Lipopolysaccharide (LPS) and the proinflammatory cytokine interferon-γ (IFNγ) to promote a classically activated M1 macrophage expressing IL-12 or conversely if exposure to IL-4 or IL-13 will promote an "alternatively activated" M2 phenotype that expresses IL-10. We predict that those studies will be completed within the next year.

In this final year, we have changed our focus in this area, based on preliminary experiments involving the toll-like receptor pathway (TLR3/4). This pathway is involved in expansion of specific myeloid cells necessary for *de novo* bone formation. Interestingly, induction of *de novo* bone formation by delivery of AdBMP2 transduced cells leads to the rapid expression of TLR3 on peripheral nerves (figure 2). This expression was noted in the tissues receiving BMP2, but not in the control (figure 2). TLR3 is a member of the Toll-like receptor family that plays a fundamental role in pathogen recognition and activation of innate immunity/myeloid cell expansion. TLRs are highly conserved from Drosophila to humans and share structural and functional similarities. They recognize pathogen-associated molecular patterns (PAMPS) that are expressed on infectious agents and mediate the production of cytokines necessary for the development of effective immunity. PAMPs activate innate immune responses, protecting the host from infection, because they tag conserved non-self molecules. For instance bacterial lipopolysaccharide (LPS), an endotoxin found on the bacterial cell membrane, is considered to be the prototypical PAMP. LPS is specifically recognized by another TLR (TLR 4). There are other components of the innate immune response including nucleotide-binding

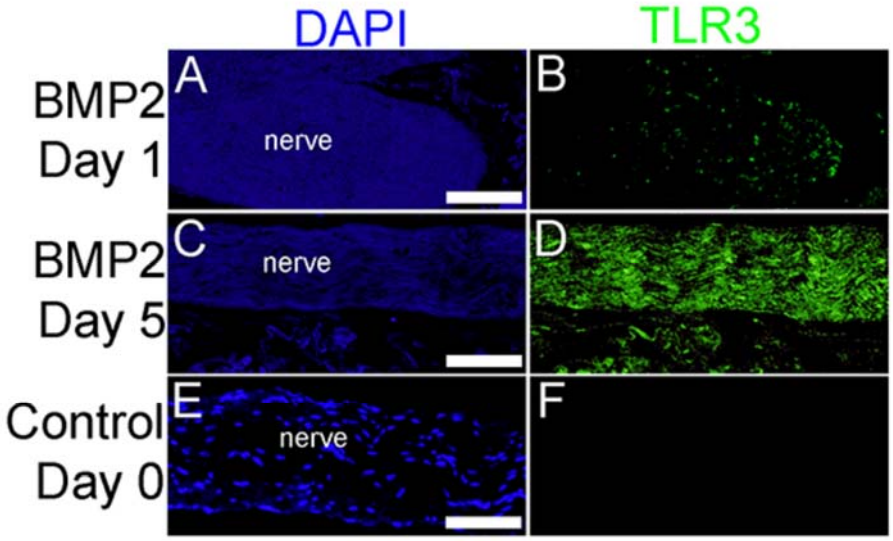

Figure 2. TLR3 is expressed in peripheral nerves after BMP2 induction. A, DAPI day 1; C, DAPI day 5; DAPI day 0; B, TLR3, day1; D, TLR3 day 5; F, TLR3, day 0.

oligomerization domain-like receptors (NOD-like receptors, NLR) and retinoic acid-inducible gene-I-like receptors (RIG-like receptors, RLR). Cytoplasmic signaling complexes, commonly called inflammasomes, are an additional component of the innate immune system. These membrane-bound (TLRs, NLRs, and RLRs) and cytosolic receptors (components of the inflammasome) are collectively called pattern recognition receptors (PRRs) because they recognize specific structural patterns. However, the specificity of innate immunity differs from that of adaptive immunity in several ways. The innate immune system recognizes structures shared by classes of microbes, whereas adaptive immunity recognizes individual details of microbes (antigens). Additionally, innate immune response has no memory, whereas adaptive immunity does. Finally, innate immunity is encoded in the germ line, whereas adaptive immunity can change because of DNA rearrangement at a somatic level. Although these distinctions are important for immune response, they may also be important in bone formation since clinical observation suggests that innate immunity favors bone formation while adaptive immunity suppresses it. However, this observation is not mechanism based, and it remains to be rigorously proven at a molecular level.

Since Toll like receptor 3's ligand is double stranded RNA, we hypothesized in these studies that TLR3/4 pathway may be activated through delivery of the adenovirus transduced cells rather than directly through the BMP2. To test this and its essential nature towards the induction of de novo bone formation, cells were transduced with the control Adempty cassette virus (AdEmpty) and then either injected alone or in the presence of 5 ug of rBMP2 without a carrier. As a control, 5 ug of BMP2 was also injected along with a collagen carrier or in the absence of any carrier or cell (figure 3). Injection with the BMP2-producing cells consistently elicits bone formation in the mouse quadriceps within 5-7 days. Because of the fact that the immune system is obviously engaged (see above) coupled with the lack of evidence that BMP2 has the ability to mobilize the immune system at physiological doses [27], we performed the following experiment. We injected 5 μg of recombinant BMP2 (rBMP2) into the mouse quadriceps, either alone or in the presence of cells transduced with AdEmpty. After 14 days HO was detected only in the mice that had received both rBMP2 as well as the AdEmpty-transduced cells. Neither rBMP2 nor AdEmpty-transduced cells administered alone resulted in detectable bone formation (figure 3). These experiments were also done in the presence or absence of a collagen sponge; surprisingly, the bone formation was suppressed in the presence of the sponge (figure 3). We did not see similar bone formation when non-transduced cells were used in place of the Adempty-transduced cells. We conclude from this preliminary experiment that innate immunity, induced by the transduced cells, is an important parameter in HO. Further, the significant inflammatory reaction created by inclusion of the collagen sponge was able to complete block the bone formation.

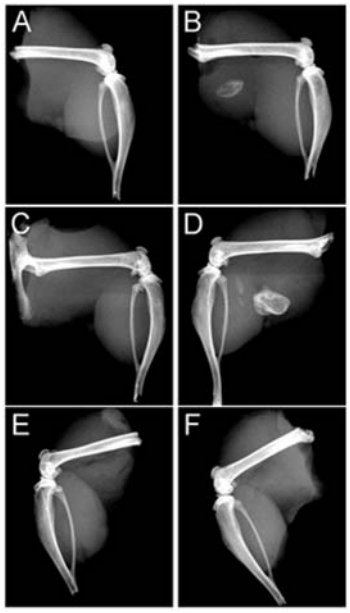

Figure 3. Ad-Empty transduced cells augment BMP2-mediated HO. A, rBMP2, 5 μg; B, rBMP2, 5 μg + AdEmpty transduced cells; C, Ad-Empty transduced cells; D, AdBMP2-transduced cells; E, rBMP2, 5 μg + collagen sponge; F, rBMP2, 5 μg + collagen sponge + AdEmpty transduced cells

The data collectively suggests that control of innate immunity potentially through activation of TLR3/4 is an essential component for BMP2 induced bone formation, and may ultimately be responsible for the generation of the mononuclear myeloid origin cells that are able to erode the mature bone for integration with the *de novo* bone. Further, these mononuclear cells appear to be precursors to the osteoclast and capable of bone resorption in the absence of fusion to form the parent cell.

Task 2: To increase the safety and controllability of the procedure through selective ablation of the cellular component of the microspheres followed by osteoclast specific resorption on the polymer, and bone healing.

We first wanted to introduce and inducible caspase 9 (icasp9$_M$) into the delivery cells so that the BMP2 production could be regulated by systemic delivery of a chemical inducer of dimerization (CID). This in turn would cause the icasp9$_M$ to become activated and initiate an apoptotic pathway leading to cell death. Therefore we generated human mesenchymal stem cells that possess a stably integrated icasp9$_M$ as well as a GFP reporter.

We also obtained an MSC cell line that does not possess the icasp9$_M$ for use as an additional control. In these first experiments we determined the timing of cell death (figure 4) and determined whether this would attenuate the BMP2 expression (figure 3). We observed immediate killing of the cells greater than 95% after exposure to the CID, however, the vehicle did not lead to any significant cell death. We next looked at BMP2 expression

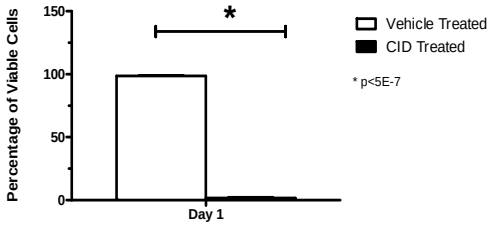

Figure 4: Cell death was immediate following delivery of the 0.1 nM chemical inducer of dimerization (CID)

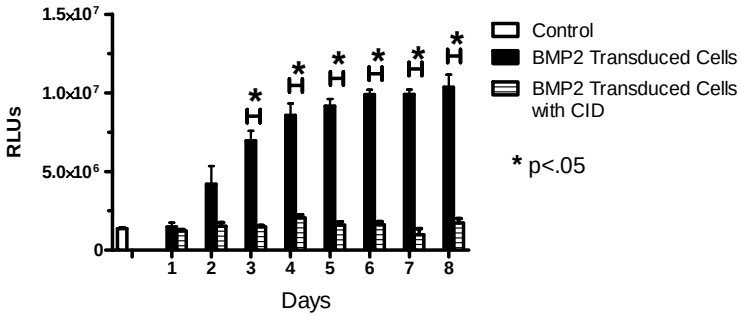

Figure 5: BMP2 activity in the presence and absence of CID. W20-17 cells were exposed for 3 days with media isolated from MSCs + icasp9$_M$ transduced with AdBMP2 (5000vp/cell) and in the presence of absence of CID. The CID was delivered on day 1, and remained in the cultures, throughout the assay. All data are reported as the mean ± standard deviation for n=3. *represents significant difference of ALP RLUs between BMP2. ($p < 0.05$).

after delivery of a single dose of CID on day 1 (figure 4). BMP2 activity was assessed through an assay in which the bone marrow cell line W20-17 will undergo osteogenic differentiation, and up regulate alkaline phosphatase activity, in presence of active BMP2. The results suggest that the single dose of CID was able to ablate the expression of BMP2 activity produced by the transduced cells (figure 5).

We next attempted to encapsulate the cells and determine if they were capable of producing BMP2 to confirm that the CID would freely diffuse into the hydrogel, and activate the icasp9$_M$ similarly to the unencapsulated cells. As seen in figure 3, images of the cells encapsulated in the hydrogel, showed a significant percentage were alive. We next looked at the ability of the encapsulated cells to undergo apoptosis in the presence of CID (figure 5). These preliminary experiments suggested that within 24 hours approximately 60-75% of the cells were observed expressing the dsRED in the MSCs + icasp9$_M$, but was reduced to approximately 40% of the cells expressing the dsRED after delivery of the 0.1nM CID. Alternatively, approximately 80% were observed expressing the dsRED in the control MSCs lacking the inducible caspase 9 regardless of the

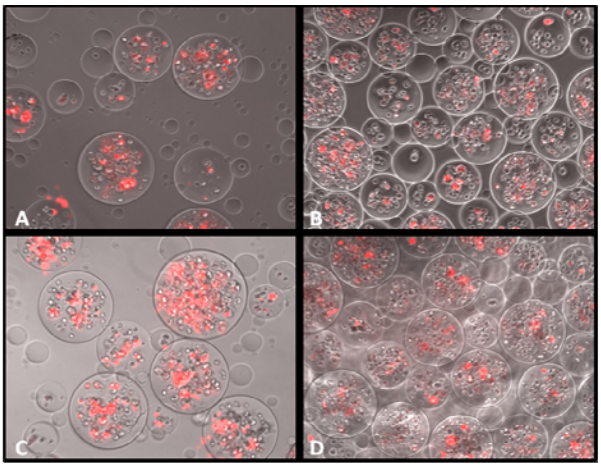

Figure 6: Comparison of dsRED expression in MSCs or MSCs + icasp9$_M$ in the presence of CID. Cells were transduced with AddsRED (5000vp/cell) and cell death was scored as the absence of red color. **(A)** hMSC-Ctrl w/o CID; **(B)** ICASP w/o CID; **(C)** hMSC-Ctrl w/ CID; **(D)** hMSC-ICASP w/ CID.

Control MSCs	**Samples with HO**
No CID	100%
CID delivered on day 1	50%
CID delivered on day 4	75%
CID delivered on day 11	50%
icasp9$_M$ MSCs	
No CID	100%
CID delivered on day 1	25%
CID delivered on day 4	25%
CID delivered on day 11	75%

Table 1: Preliminary analysis of the HO in the presence or absence of CID in MSCs and MSCs + icasp9$_M$

presence of CID. Although preliminary these studies suggest that the CID is able to induce apoptosis in the encapsulated cells. Further studies are ongoing to follow up and optimize the kinetics and delivery of CID to the encapsulated cells.

We next attempted to encapsulate the cells and determine if they were capable of producing BMP2 to confirm that the CID would freely diffuse into the hydrogel, and activate the icasp9$_M$ similarly to the unencapsulated cells. As seen in figure 6, although the preliminary data appears to be variable. These preliminary experiments suggested that within 24 hours approximately 60-75% of the cells were observed expressing the dsRED in the MSCs + icasp9$_M$, but was reduced to approximately 40% of the cells expressing the dsRED after delivery of the 0.1nM CID. Alternatively, approximately 80% were observed expressing the dsRED in the control MSCs lacking the inducible caspase 9 regardless of the presence of CID. Although preliminary these studies suggest that the CID is able to induce apoptosis in the encapsulated cells. Further studies are ongoing to follow up and optimize the kinetics and delivery of CID to the encapsulated cells.

We also performed a very preliminary study to look at whether delivery of the CID could then suppress bone formation *in vivo*. In these studies, the MSCs or MSCs + icasp9$_M$ were transduced with AdBMP2 (5000vp/cell) and then injected into the rear hind-limb of NOD/Scid mice. Bone formation was detected using x-ray approximately 15 days after the initial injection (figure 6). Although there was significant variability within groups (Table 1), the trends suggest that deliver of the CID was able to suppress the bone formation when delivered earlier in the reaction (figure 6, panels A and B). However, when delivered at 11 days after initial induction of HO, the majority of the samples had significant HO (figure 6, panel C).

Since analyzing the bone formation is an outcome of the potential activation of the safety switch we chose to look more directly at whether we are able to terminate the cells through delivery of CID. In these experiments, the MSCs + icasp9$_M$ were transduced with both AdBMP2 (5000vp/cell) and AdiRFP (2500 vp/cell) which is a fluorescent near infrared protein that can be readily detected through near infrared imaging. A portion of the cells were encapsulated while another portion was directly injected into the mice. The mice were then separated into two groups one that received two injections of the CID and the other vehicle. The two injections were not varied within this group but were initiated on day 0 or time of induction of bone formation with the following given 24 hours later. The near infrared signal was then visualized and quantified every other day by NIR imaging (figure 7). In the leg which received the cells directly, there was an obvious attenuation of the signal in the presence of CID as compared to the mice that did receive the vehicle. It was not

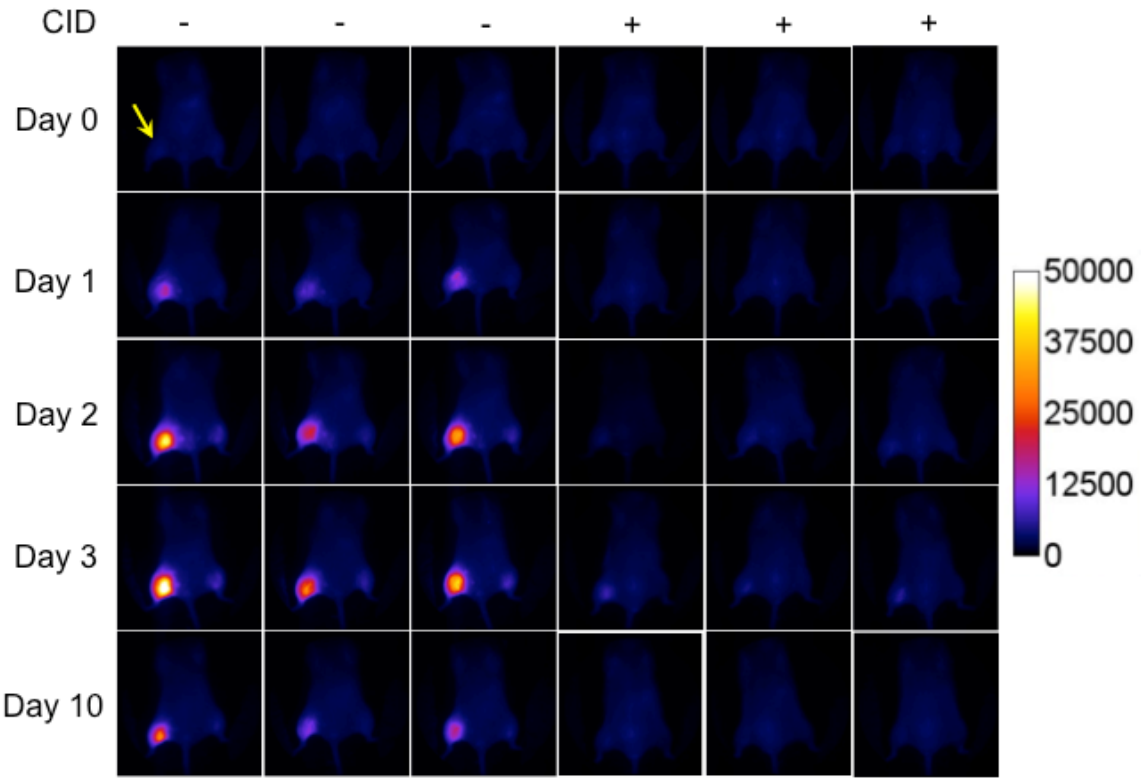

Figure 7: Far-red fluorescent intensity of AdBMP-2 transduced hMSC-iCasp9 cells expressing a far-red fluorescent protein over time in NOD/SCID mice. hMSC-iCasp9 cells were transduced with an AdiRFP (2500 vp/cell) and AdBMP2 (5000vp/cell). The right leg (yellow arrow) received the cells directly; whereas the left leg received the PEGDA hydrogel encapsulated cells.

surprising that the signal appeared to increase between day 1 and 2, since adenovirus expression of the protein is still occurring and has not reached steady state. Each animal (n=3) was imaged over the course of bone formation. Unfortunately, it appears that the PEG-Da hydrogel material appeared to shield the iRFP signal as compared to the un-encapsulated animals. However, this method was sensitive enough to be able to quantify changes in the expression even in the legs receiving hydrogel. Results of the quantification are shown in figure 8. Since these adenovirus transduced cells also were expressing the BMP2, bone formation was quantified in each group. Representative images are shown in figure 9. The results show that both the limb that received the encapsulated AdBMP2 transduced cells and the limb that received the directly injected AdBMP2 transduced cells produced bone, whereas in the presence of CID, regardless of the encapsulation, no bone was observed, suggesting the drug had terminated the reaction.

We next wanted to look at the timing of delivery of the CID. In these experiments, the CID was delivered at various time points after induction of bone formation with the AdBMP2, AdiRFP transduced cells. The original data was collected when the CID was delivered at days 0-1, so the new points were day 2-3, day 4-5, day 6-7, and day 8-9. We chose to vary the timing of delivery to see if it would stop the bone formation or impact it in any way. Obviously, if one chose to use this system to stop the BMP2 induced bone formation, there would potentially be a point at which the formation would continue even in the absence of the cells. Alternatively, the proposed aim was to be able to remove the cells after the bone formation without altering the newly forming bone. The results of this imaging on bone formation are depicted in figure 10. MicroCT analysis showed that when delivered on day 2-3 the process was completely blocked, whereas on day 4-5 some bone formed but it appears attenuated. We are currently quantifying the results. When the CID was delivered at a point during the assay where early bone is already being deposited, it had no effect overall. In all cases delivery of the CID attenuated the iRFP signal.

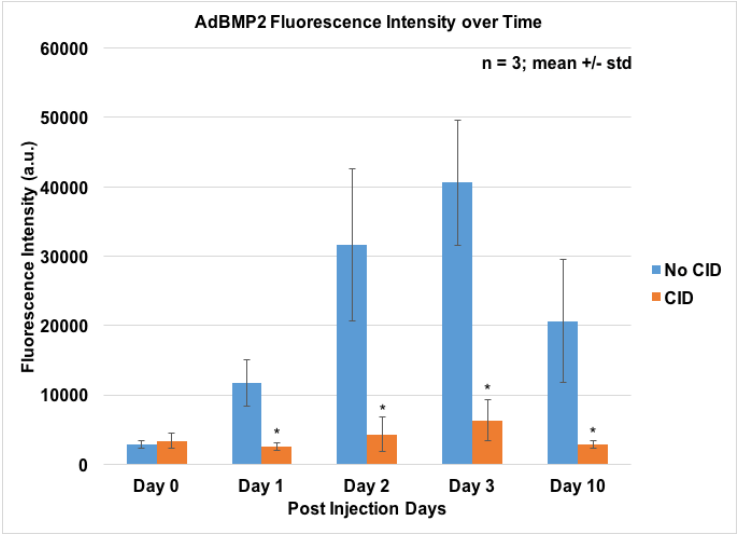

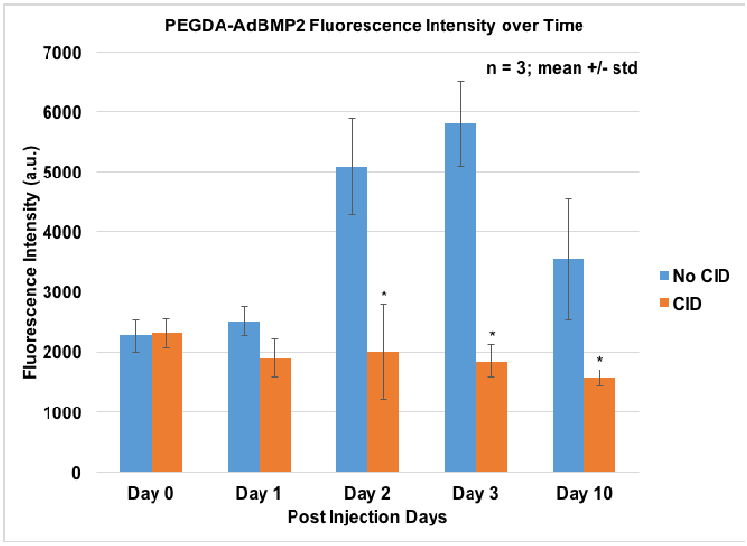

Figure 8: Far-red fluorescence intensity over time in hind limbs of NOD/SCID mice receiving AdBMP-2, AdiRFP transduced hMSC-iCasp9 cells in the presence or absence of chemical inducer of dimerization (CID). The right leg of the mouse received the unencapsulated cells while the left received the same number of transduced cells encapsulated in a PEGDa hydrogel microsphere. All data are reported as the mean ± standard deviation for n=4. *represents significant difference of fluorescence intensity between cells and cells treated with a chemical inducer of dimerization (CID) ($p < 0.05$).

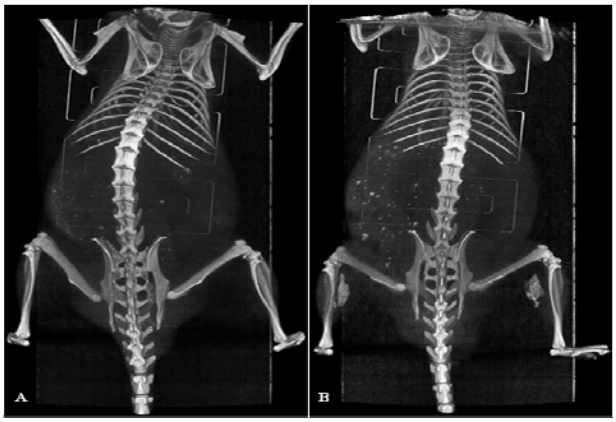

Figure 9: Representative microCT images of the groups that received CID (Panel A) versus those that did not receive CID (Panel B). Left leg received the PEGDa hydrogel, while the right leg received the cells directly injected.

The data collectively shows that we can utilize the switch to safely remove the cells during the degradation of the hydrogels, and that the removal of the material will not adversely affect the newly formed bone. Alternatively, the experiments also show that BMP2 must be present until mature cells form cartilage and bone matrix. This is consistent with BMP2's role in inducing chondro-osseus differentiation of progenitors. Further, this highlights the importance of the adenovirus transduced cells that are capable of secreting BMP2 over the course of several days to a week at the target location.

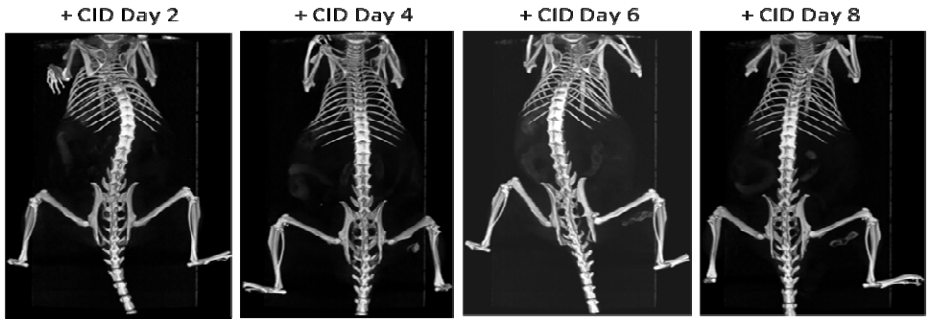

Figure 10: Representative radiographs collected from microCT analysis of bone formation at 2 weeks after delivery of AdBMP2, AdiRFP transduced hMSC-iCasp9 cells into one hind limb. The days represent the first day of the two consecutive injections of CID that were given to the NOD/Scid mice.

Task 3: To assess and compare bone quality of the skeletal and new bone during and after completion of the fusion.

To accomplish this, we have developed a non-invasive optical imaging methodology to determine the optimal dose of microspheres with respect to their placement, cell viability and resultant bone formation. Therefore we altered our approach by incorporating an Alexafluor dye into the PEG hydrogel that could be detected optically. To further confirm viability of the cells, we transduced the cells with AdIFP and AdBMP2, so that we could follow the cells. Initial experiments were performed to then detect the presence of the two reporters with respect to the newly forming bone. Since this involved both optical imaging and co-alignment with microCT, we had to develop novel methodology to integrate the systems. These experiments lead to a publication of this methodology (see appendix). We propose in the next year to implement this technology using a newer reporter virus that does not interfere with the BMP2 expression, and will provide more robust bone formation. Further we will also add microPET imaging for early bone formation through detection of MMP9, which we have previously shown highlights the region where the bone matrix will be placed. From these initial findings we observed the critical nature of placement of the materials, and this work has been published.

Unfortunately however, we did not observe spine fusion in the rat. In fact the bone formation was very poor as compared to the mouse and often its formation was highly variable. This was surprising because in many studies when placed near either the fibula or femur in rats the therapy worked extremely well. These results were independent of immune responses to the adenovirus transduced cells, since similar results were obtained when the cells were encapsulated in PEGDA hydrogel [20], which prevents immune detection (see next section), or performed in athymic rats lacking B and T cells. Since we were unable to move forward until we overcame this obstacle we decided compare the process of bone formation between the rat and mouse. However, first we had to reliably obtain *de novo* bone formation in the rat. For these studies we decided to go back to our standard assay, where we observed the process working well in skeletal defects in either the limb[1] or femur [2]. Surprisingly, we noted that it did not work at all when placed in the muscle at a location distal from the intact skeleton; however, when the cells were injected adjacent to the intact skeletal bone, robust bone formation was observed (figure 11). Further, if we injected cells adjacent to the skeletal bone, and then in a separate leg distal, we still could not recover the bone formation, suggesting that if there was a circulating progenitor, it was not able to recruit to the "distal" site. However, if we were to inject into the rats at site proximal to the skeleton and then inject a second time at a distal site, heterotopic bone formation occurred at bone locations, suggesting that the site in the muscle could support the bone formation.

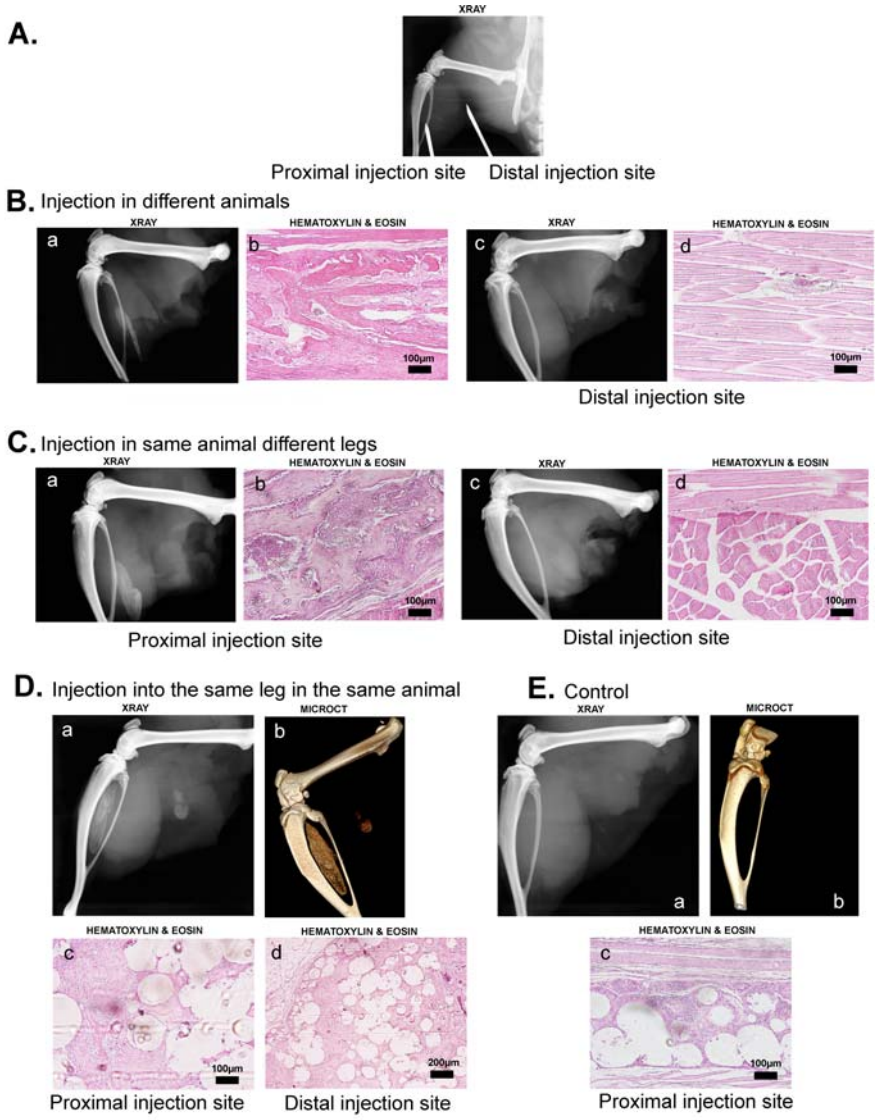

Figure 11: Detection of Heterotopic Ossification (HO). Radiographic and histological analysis of tissues isolated two weeks after induction of HO. **A.** Representative radiograph showing the location of the distal versus proximal injection sites. **B.** Representative radiographs and photomicrographs of tissues isolated from Wistar rats two weeks after receiving either a proximal or distal injection of AdBMP2 transduced cells. **C.** Representative radiographs and photomicrographs of tissues isolated from a single Wistar rat 2 weeks after receiving a proximal injection of AdBMP2 transduced cells and a distal injection of the same cells in the contralateral limb. **D.** Representative radiograph, microCT image, and photomicrographs of tissue isolated from a single Wistar rat two weeks after receiving a proximal and distal injection in the same limb of microencapsulated AdBMP2 transduced cells. **E.** Representative radiograph, microCT image and photomicrograph of tissue isolated two weeks after injection of Adempty transduced cells.

Thinking that potentially we mobilized a progenitor population in the rat when delivering the cells to both locations, we next delivered the AdBMP2 transduced cells at the distal location, along with 1 x 10^6 human mesenchymal stem cells (MSCs), which we had previously shown to incorporate into the structures of bone and cartilage, when added in a similar fashion in the mouse. Surprisingly, they were unable to rescue the bone formation, suggesting that additional factors or cells must be lacking that are necessary to produce the bone (figure 12, panel A). However, these human MSCs when injected along with AdBMP2 transduced cells in NOD/Scid mice, led to their incorporation into mesenchymal structures, including cartilage, bone and adipose (figure 12 panel B).

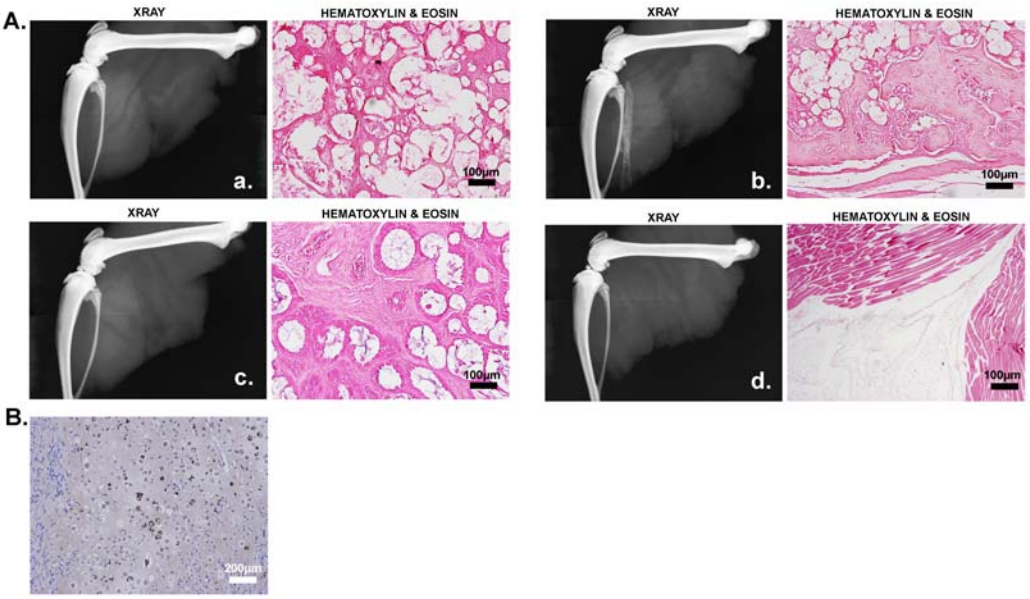

Figure 12: A. Radiographic and histological analysis of tissues isolated two weeks after induction of HO in the presence and absence of hMSCs. Wistar rats were injected at the distal **(a)** or proximal **(b)** location with AdBMP2 transduced cells and the distal location with hMSCs + AdBMP2 transduced cells **(c)** or hMSCs + PBS **(d).**
B. Photomicrograph of mouse tissue isolated 2 weeks after induction of HO by delivery of AdBMP2 transduced cells in the presence of hMSCs. The differentiation of the hMSCs into mesenchymal tissues of bone was confirmed through immunostaining with an antibody that specifically detects the human cells (brown). The representative section shows the presence of human chondrocytes within the mouse bone.

We next looked at the progenitors that responded in the rat, and compared them with the progenitors that respond in mice (figure 13). The osteoprogenitors were identified as osterix positive cells. These cells appeared to express similar markers as the mouse, both being claudin 5 and PDGFRα positive (this data not show, see appendix). However, in the mouse, the cells appear to be derived from the peripheral nerves [3,4,5], whereas here we noted that they were migrating from the periosteum, similar to a periosteal reaction. When the AdBMP2 transduced cells were injected both close and distal the cells that had migrated towards the BMP2 at the proximal location were able to continue to migrate towards the distal site. We have previously demonstrated a role for stem cells within the peripheral nerves to contribute to the *de novo* bone formation[3, 4, 5]. Surprisingly, almost no osterix expression was observed in the peripheral nerves of the rats 24-48 hours after delivery of the AdBMP2 transduced cells, whereas at later days the entire nerve appeared to be expressing claudin 5 and osterix (figure 14). The data suggested that perhaps a similar cell population was undergoing osteogenesis in the presence of the BMP2, but unable to exit the nerve.

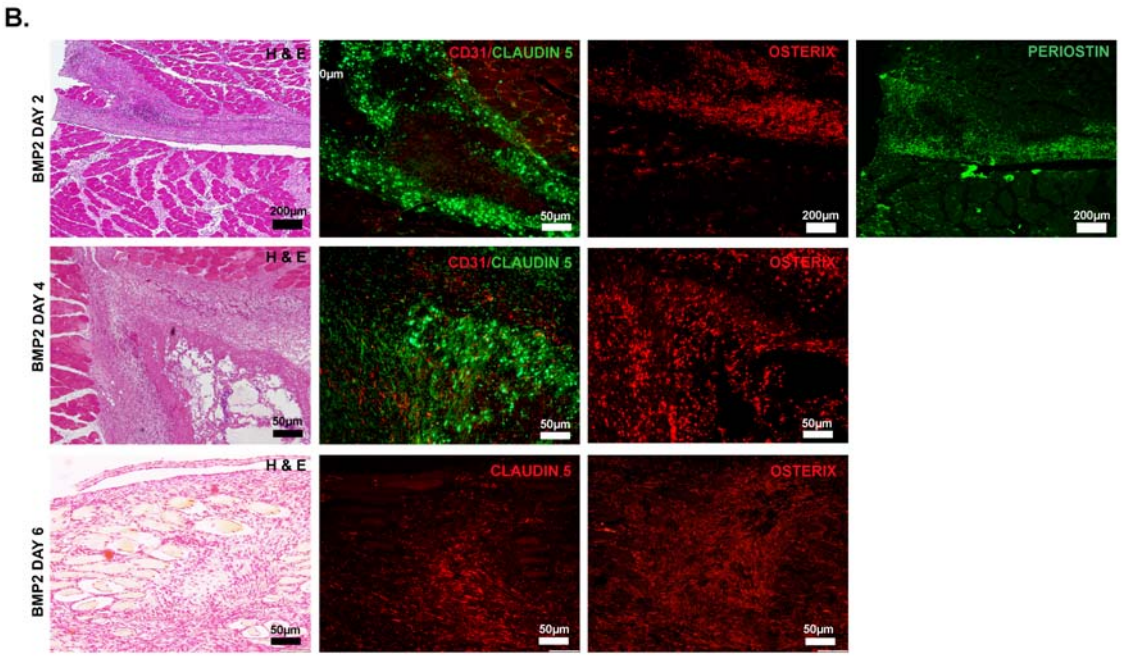

Figure 13: B: Osterix and claudin 5 expression in the periosteum of the fibula near site of HO. Serial paraffin sections, every 10th slide, were hematoxylin and eosin stained to locate the region of bone formation. Unstained serial sections were then immunostained for osterix (osteoprogenitors). Serial sections were also co-immunostained with claudin 5 and CD31 to determine if the cells expressing claudin 5 were associated with the vasculature and periostin to confirm that the cells were associated with the periosteum.

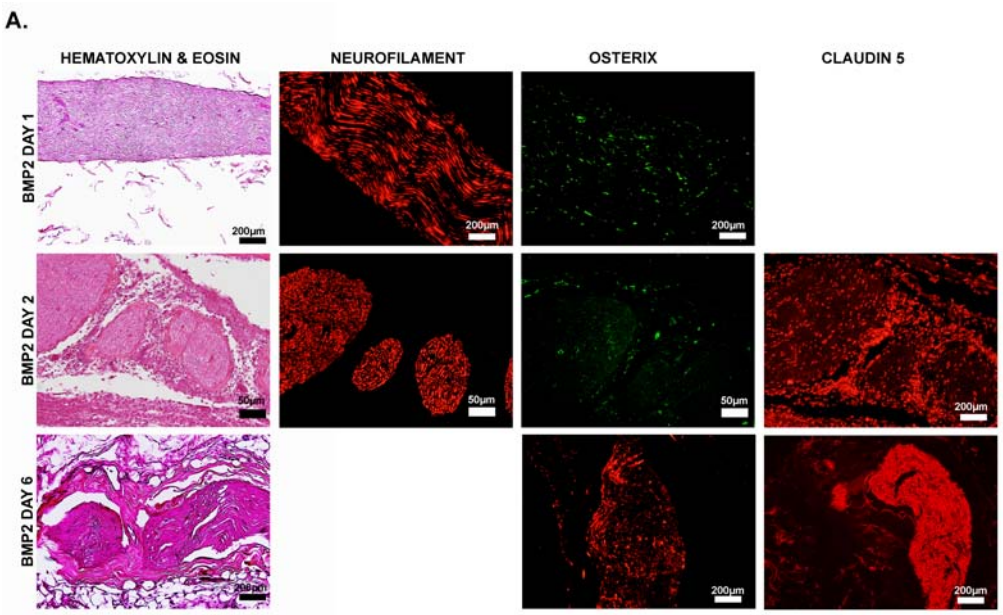

Figure 14: Representative photomicrographs of immunohistochemical staining of tissues isolated 1, 2, and 6 days after a proximal injection of AdBMP2 transduced cells.
A. Osterix and claudin 5 expression in peripheral nerves within the area of HO. Serial paraffin sections, every 10th slide, were hematoxylin and eosin stained to locate the region of bone formation. Unstained serial sections were then co-immunostained for neurofilament to detect the nerve and the osteogenic factor osterix. Additional sections were also immunostained for claudin 5 an osteogenic marker in mice.

The inability of the cells to exit the nerve suggests that they may not be able to cross the blood nerve barrier in rats and thus, unless adjacent to a large enough region of innervated periosteum, bone formation will not occur. Therefore, we next looked for factors that are known to be involved with temporarily opening of the barrier. One of the best described is activated MMP9, which can function in complex with claudin 1 to temporarily alleviate some of the constraints on the barrier. We previously showed that activated MMP9 was associated with peripheral nerves adjacent to the site of bone formation and significantly elevated both at the RNA and protein level in tissues undergoing BMP2 induced bone formation[6]. Tissues were then isolated during bone formation and protein extracted to look both at total protein (active plus inactive) and activity. The results suggested that MMP9 is slightly elevated on day 4, but then quickly returns to control levels (Figure 15). Total protein was elevated on day 2, although the control tissues, which received Adempty cassette transduced cells were also elevated and then significantly elevated on day 4, but then dropped drastically by day 6, rather than staying elevated as in the mouse. Immunohistochemical staining suggested that the majority of the protein was in the inactive precursor state rather than activated unlike the mouse (Figure 15).

The activation of MMP9 requires a cleavage step of the pro form for activation. This cleavage requires MMP3, which has been shown to be present in subsets of blood cells, and adipose progenitors. MMP3^{+} staining is observed in the mouse associated with the UCP1^{+} brown adipose, whereas in the rat it appears to be in cells adjacent to the tentative brown adipose (data not shown). MMP3 must also undergo a conformational change similar to MMP9 for activation by plasminogen (Figure 16).

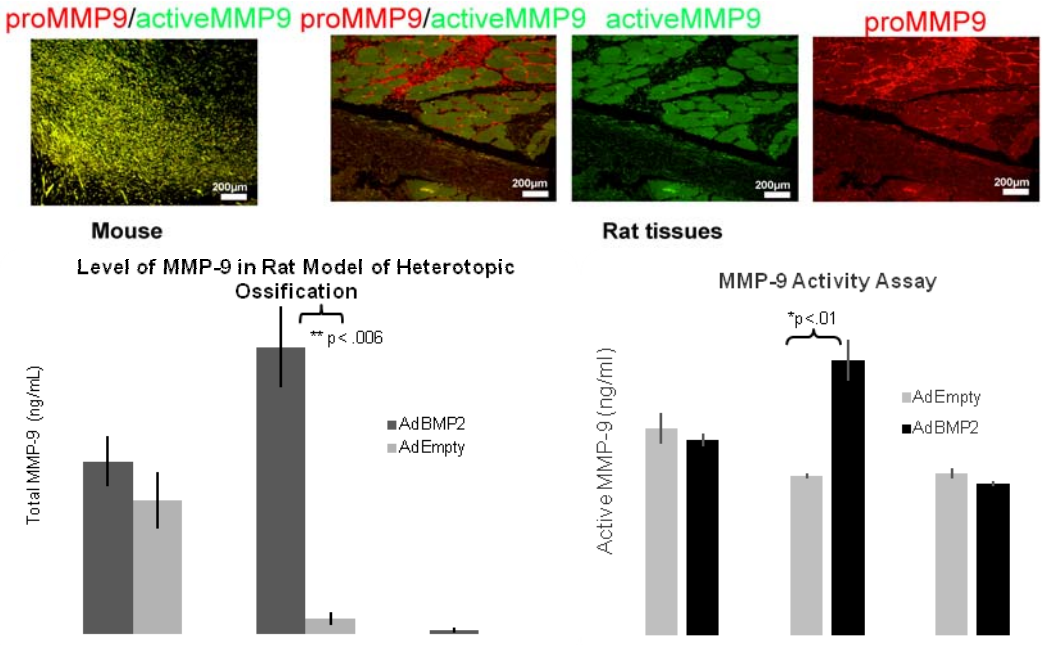

Figure 15: Detection of MMP9 total protein and active MMP9 in rat tissues. Representative photomicrographs of paraffin sections serially cut from mouse or rat tissues isolated at the site of *de novo* bone formation. Tissue sections were co-immunostained with antibodies that detect both active and inactive forms of MMP9 (red) or only the active form (active). Tissues were isolated from rats at 2, 4, and 6 days after close injection of AdBMP2 and Adempty transduced cells and protein extracts generated. **A.** MMP-9 protein was bound through ELISA, and then substrate added, to quantify MMP-9 functional activity. **B.** MMP9 total protein was bound through ELISA and quantified directly. Statistically significance was calculated using a standard t-test, with n=6.* denotes statistical significance.

Plasminogen is made in the liver and deposited in the blood stream where it immediately binds to platelet membranes and remains inactive. During platelet activation platelets undergo a conformational change and expose the plasminogen for cleavage by urokinase or tissue plasminogen activator. We note that in both mouse and rat tissues after induction of *de novo* bone formation, brown adipocytes express high levels of urokinase (data not shown). Preliminary data suggests that platelets in the mouse decrease after induction of *de novo* bone in the blood, whereas the rat platelets increase in the blood (Figure 17). Plasminogen levels in the rat tissues did not change, whereas in mouse it increased by 200 fold (Figure 17). It is unclear why platelets do not appear to recruit to the site of bone formation resulting in the absence of plasmin in rats.

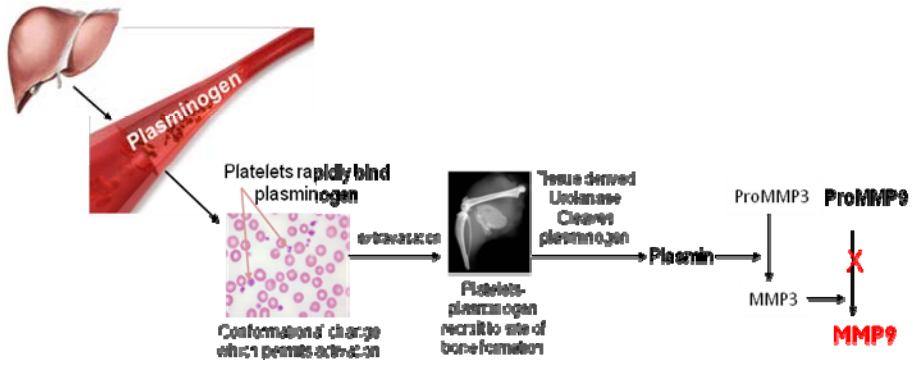

Figure 16: Schematic of the mechanism of MMP9 activation

The data collectively suggests that MMP9 does not become active as in the mouse, but in order to determine if this could be responsible for the lack of de novo bone formation observed in the rat at the distal location, we next suppressed MMP9 in mice and measured the changes in heterotopic bone formation. Mice received either intraperitoneal injections of minocycline, a tetracycline derivative that has been reported to suppress MMP9, or vehicle, and then AdBMP2 transduced cells in the hind limb, and bone formation allowed to progress for two weeks. Bone formation was quantified by measuring total bone volume in the rats at two weeks (Figure 18). BMP2 induced bone formation in the mouse was significantly inhibited with suppression of MMP9. The mechanism of minocycline is unknown; however, analysis of the tissues suggests that it blocks MMP9 activation rather than

protein production. We are currently looking towards delivery of active MMP9 to the rat to determine if we can rescue the heterotopic bone formation.

The data suggests that in rat, BMP2 must mobilize osteoprogenitors from the periosteum, rather than peripheral nerve. So in addition to the previous experiments we are attempting to rescue the bone formation through direct delivery of the isolated neural derived osteoprogenitors. Presumably there is a lack of responsive periosteum associated with the skeletal vertebra to permit the proximal HO observed in the rat hind limb. Further, without harnessing the neural derived process, spine fusion was unobtainable. It is unclear why the rat did no launch a similar process as in mice. Since activation of platelets for MMP9 activation requires specific inflammatory cascade to be active, we next chose to look at whether we were launching an immune response against the adenovirus transduced cells. Although we observed similar findings in athymic rats which lack B and T cells, we questioned if immunity is playing a functional role in the bone formation, then alteration of these immune pathways, through delivery of the foreign adenovirus transduced cells could be affecting the process. One potential problem is that adenovirus are a family of viruses, that have specific strains that can affect a number of different species, and may potentially have some immunological overlap leading to immune priming of the species. Mice are unique in that there are really no virus strains that have similarities to the human adenovirus type 5, therefore it will not have any immunological priming.

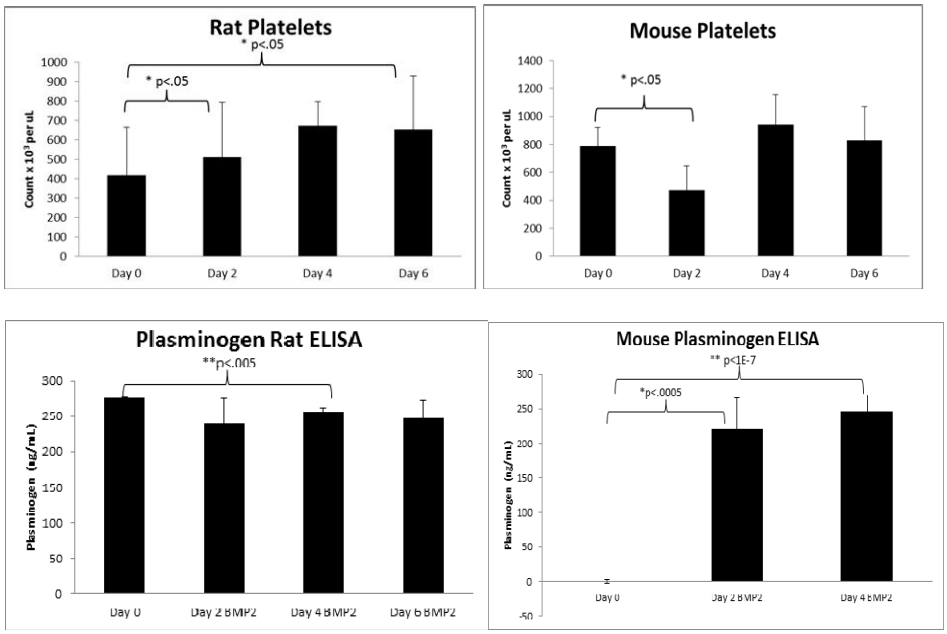

Figure 17: Quantification of platelets number and plasminogen/plasmin protein levels in mouse and rat tissues. Blood platelets were quantified in mouse and rat blood isolated at indicated days. The significance is indicated in figure. Total protein was isolated from soft tissues surrounding the site of new bone formation in rat and mouse and plasminogen/plasmin quantified using a standard ELISA. Statistical significance was determined by a one way ANOVA with a Tukey- Kramer post-hoc test with confidence interval of 95% ($p<0.05$). * denotes statistical significance.

Alternatively, rats are not as inbred and may in fact have some virus strains that could cross protect the organism from the adenovirus transduced cells. To assess the role that immunological memory may play in this process, we set up the following set of experiments.

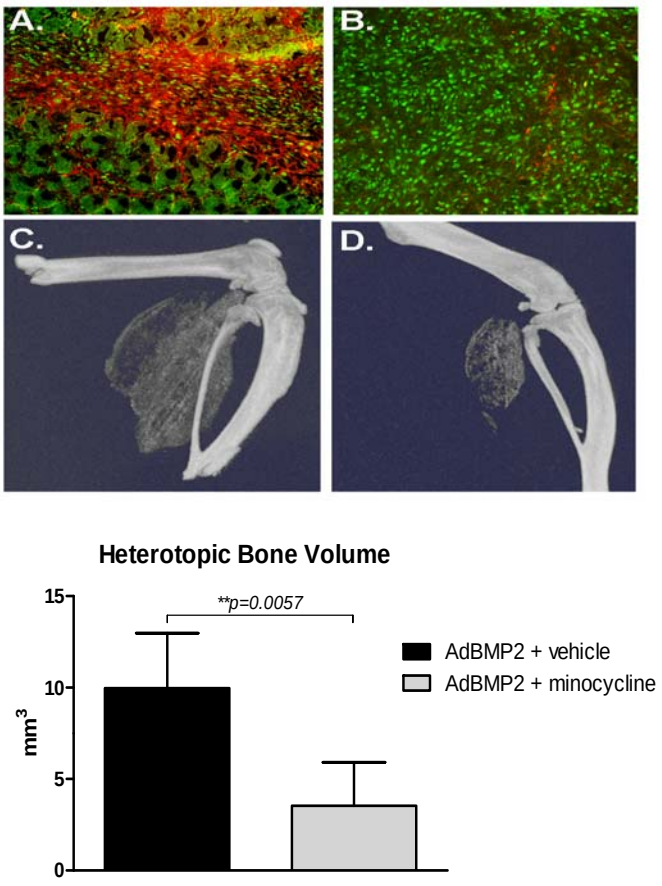

Figure 18: Quantification of HO in mice treated with minocycline or vehicle. Mice were treated with minocycline or vehicle and HO induced through delivery of Ad5BMP2 transduced cells. (**A**) Tissues were analyzed at 4 days for the presence of both total MMP9 (green color) and active MMP9 (red color) expression. (**C and D**) Bone formation was quantified in tissues isolated 14 days after induction of HO and three dimensional reconstruction of the resultant bone is depicted. (**E**) Bone volume was then calculated from each animal (n=4) and the average volume and standard error of the mean depicted. Statistical significance was determined by student t-test with confidence interval of 95% ($p<0.05$). * denotes statistical significance.

Although our system does not involve providing live virus to the mice, potential adenovirus capsid and fiber proteins may be associated with the cells enough to launch a response. To look at this, Adempty cassette transduced cells, PEGDa hydrogel encapsulated Adempty cassette transduced cells, or vehicle (PBS) was injected into the mouse hind limb. Approximately 1 week later, AdBMP2 transduced cells were then injected into the contralateral limb, and bone formation allowed to progress for two more weeks. As expected if the mice (n=4) received an injection of PBS one week prior to receiving the AdBMP2 transduced cells either encapsulated or directly injected, progressed as expected, with significant bone observed by x-ray two weeks later (figure 19, Panels A and C). However, when the mice were injected with Adempty cassette transduced cells in place of the PBS, and the BMP2 induced bone formation, induced one week later by injection in the contralateral limb of AdBMP2 transduced cells, was completely ablated (figure 19, Panel B). The experiments suggested that exposure to the Adempty cassette transduced cells was able to wipe out the ability for the AdBMP2 transduced cells to induce bone formation one week later in the opposite limb. Since the PEGDa-hydrogel has been previously shown to protect cells from immune clearance, we next encapsulated the AdBMP2 transduced cells in the hydrogel and injected them one week after priming with the Adempty cassette transduced cells (figure 19, Panel D). In all cases the bone formation was restored in the limb, suggesting that the hydrogel could prevent the detection of the adenovirus transduced cells. We next encapsulated the Adempty cassette transduced

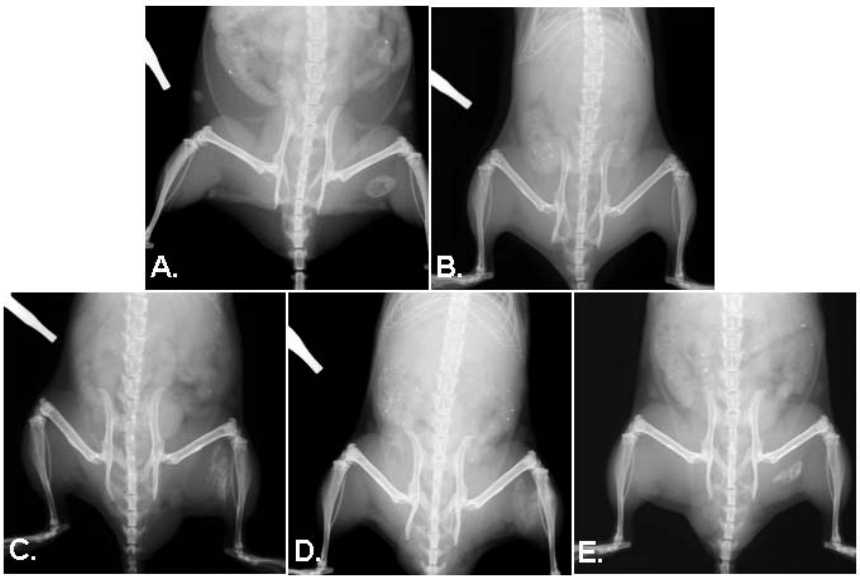

Figure 19: Representative X-rays of mouse hind limb 2 weeks after induction of bone formation by delivery of AdBMP2 (Panels A., B., E.) or AdBMP2 – PEGDa hydrogel encapsulated cells (Panels C, D) and three weeks after injection in the contralateral limb of Adempty cassette transduced cells (Panels B, D) Adempty cassette transduced cells encapsulated in hydrogel (E), or PBS (A, C).

experiment, a constant amount of adenovirus was exposed to varying amounts of the sera or in the case of the control (PBS) for 30 mins, prior to adding the virus to human 293 cells (cells known to possess the adenovirus CAR receptor). The virus was then allowed to infect the dishes, and 48 hours later infected cells were identified using a rapid titer kit. As expected the sera from animals that received PBS had similar infectious titers (no significant difference) in this assay as the control virus alone, suggesting that they do not possess antibodies to the adenovirus (figure 20). Alternatively we observed a significant reduction both in the mouse and rat sera that had received adenovirus transduced cells two weeks prior to sera collection. Alternatively, the mice that received the adenovirus encapsulated cells were not statistically different from the control, again demonstrating that the PEG-Da hydrogel was able to prevent antibody production in the mice against the injected materials. Interestingly, all the mouse sera samples appeared to be trending lower than the adenovirus control, suggesting that perhaps there were nonspecific inhibitors of the virus in the animal's blood in general.

One final experiment to demonstrate that humoral immunity is involved in the ablation of BMP2 induced bone formation; we next set up the same experiments in NOD/Scid mice, which lack B and T cells (figure 21). As predicted prior exposure to the adenovirus transduced cells (Adempty cassette transduced cells) does not suppress bone formation when the cells are directly injected. These results demonstrate that prior exposure (priming) to the adenovirus even when no free virus is used, can totally suppress the bone formation. Alternatively, it also clearly demonstrates that encapsulation of the cells in the PEG-Da hydrogel can overcome these challenges, and is a necessary and important component to this cells in a PEG-Da hydrogel (figure 19, Panel E) and then directly inject cells into the contralateral hind limb one week later. As seen in figure 19, Panel E bone formation progressed as expected.

We next chose to confirm that the loss in bone formation after prior exposure to adenovirus transduced cells in mice was due to immunological priming, where antibodies have been made against the foreign materials. Therefore serum was isolated from these mice, two weeks after the injection of either AdEmpty transduced cells , PEG-Da hydrogel encapsulated Adempty transduced cells or vehicle (PBS). To determine if the mice made antibodies against the materials injected (Adempty transduced cells, encapsulated Adempty transduced cells, and PBS) sera was collected, and assayed for antibodies that could neutralize adenovirus. In this

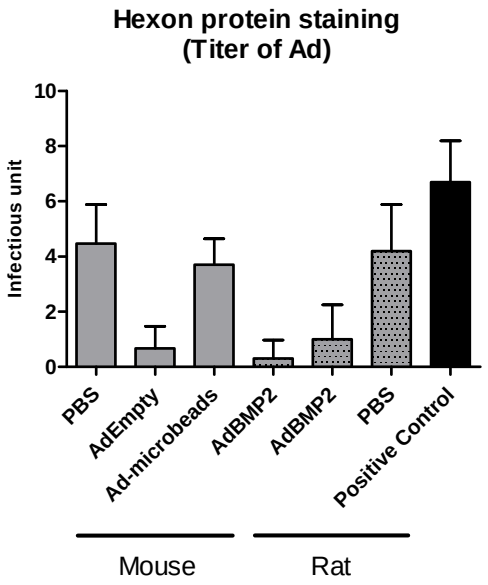

Figure 20: Neutralizing antibody levels in mouse (n=3) serum after exposure to AdEmpty transduced cells either directly injected or encapsulated with a PEG-Da hydrogel prior to injection or PBS (control). Serum was then subject to 10 fold dilutions and mixed with a constant amount of adenovirus. The mixture was then placed on 293 cells, and viral titers were determined using a rapid titer kit (clonetech). Statistical significance was determined by a one way ANOVA with Tukey post-hoc correction test with confidence interval of 95% ($p<0.05$). * denotes statistical significance.

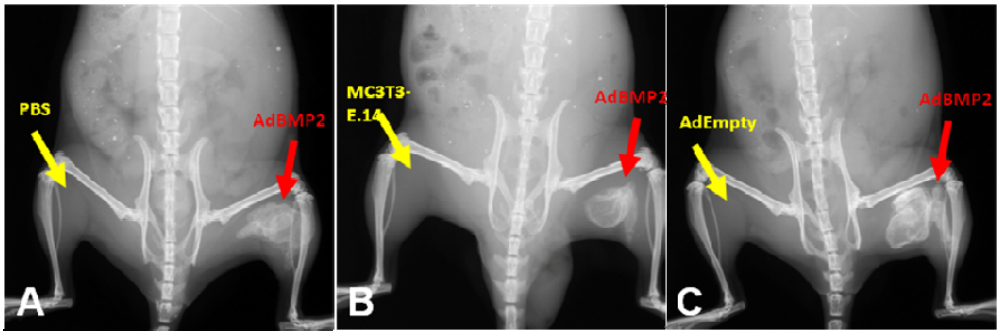

Figure 21: Representative X-rays of mouse hind limb 2 weeks after induction of bone formation by delivery of AdBMP2 transduced cells (red arrows) and one week after delivery of either (PBS, cells alone (MC3T3E1), and Adempty transduced cells; yellow arrow).

process.

CONCLUSION:

We have performed experiments to isolate and characterize the potential M2 monocyte cells that we propose are involved in rapid remodeling of the skeletal bone matrix for integration to the newly formed bone fusion mass. We have sought to identify the cells and molecular pathway that has led to the production of the mononuclear cells observed to be absorbing the newly formed bone at the site of spine fusion. Through these experiments it appears to be similar to the parent mononuclear cell that fuses to form the osteoclast. Further, experiments to investigate the role of myeloid progenitors in the bone formation process, led to our finding the toll like receptors may play a key role in the formation of bone. These pathways appear to be active and necessary for robust BMP2 induced bone formation. These findings that TLR pathways are essential to BMP2 induced bone formation is novel, and the subject of a patent disclosure. Additionally, the regulation of this pathway with respect to generation of the mononuclear osteoclast-like cells is still unknown.

We have now demonstrated both the necessity of the PEGDa hydrogel encapsulation of the adenovirus transduced cells, but also that inclusion of the icasp9M, allows for selective induction of cell death, and stopping of BMP2 induced bone formation. Further, bone formation prior to the presence of mature cells and matrix requires the presence of BMP2. If the cells are removed early, then bone formation is attenuated. This will provide an important safety switch for surgeons to ensure bone formation is appropriate and in the correct space. The data taken together, suggests that the AdBMP2 transduced cells encapsulated in the PEGDa hydrogel will be very effective at inducing targeted bone formation. However, surprisingly in the rat, this was not the case. In these experiments, we noted that bone formation would only progress when near the skeletal bone. The finding occurred even when the cells were encapsulated in the PEG-Da hydrogel, so could not be explained by humoral immunity. However, a comparison of the processes showed a significant change occurred with the activation of MMP9. If MMP9 either did not get activated (rats) or was suppressed in mice, heterotopic bone formation was suppressed. Further, this appears to be a result in the lack of active plasmin/platelets in the tissues. It is unclear why the biology of the rat appears to be different, but led us to question what happens in humans. To this end we obtained all appropriate approvals to start to look at heterotopic ossification in humans. Preliminary data suggests that in the humans MMP9 is all in the active state. Therefore the data collectively, suggests that perhaps several of these large animal models may not reflect the humans. Alternatively, there may also be a necessary second component to the BMP2, which is required for robust bone formation. This second component may be active in the mouse and in humans undergoing heterotopic ossification (after traumatic injury), but lacking in other species, and perhaps humans with skeletal fractures not undergoing HO. One likely candidate is TLR3/4, where our early experiments suggest it can activate key pathways that allow for even low dose recombinant protein to work efficiently in mice.

These FINDINGS are critical to developing a safe and effective low dose model of harnessing BMP2's ability to launch *de novo* bone formation. Although dissecting this process may appear to lack translational focus, it is an essential component to any conversations with the FDA in the future, as to the appropriate large animal model. Since this is the development of a biological, knowing the essential components, and understanding the biology in mice, large animals, and humans will be imperative for successful translation into the clinic. **We have taken a major step forward in the field by identifying a tentative second pathway and component, and demonstrating its potential essential nature in harnessing BMP2 *de novo* bone formation in any species. Further, understanding the role of immunity and clearly demonstrating that we can easily overcome this aspect of the therapy is also a major finding.** This work

will be relevant to all individuals that wish to utilize BMPs as osteoinductive agents, and are the start of demonstrating how to reliably induce bone formation at a target site.

REFERENCES:

1. Lazard ZW, Heggeness M, Olabisi RM, Hsu C, Hipp JA, Gannon F, Davis AR, West JL, and Olmsted-Davis EA. Cell Based Gene Therapy for Repair of Critical Size Defects in the Rat Fibula. J Cell Biochem. 2011 Jun;112(6):1563-71. PMID:2134448.
2. Sonnet C, Olabisi R, Simpson C, Weh M, Peroni J, Gugala Z, Hipp JA, Gannon FH, Lindsey RW, Davis AR, West JL, and Olmsted-Davis EA. Injection of Osteoinductive Microspheres Leads to Rapid Healing of Critical Size Femoral Defects in Wild Type Rats. J. Orthop Res. 2013 Oct;31(10):1597-604.
3. Salisbury EA, Rodenberg E, Sonnet C, Gannon F, H. Shine D, Vadakkan T, Dickinson M, Olmsted-Davis EA, and Davis AR. Sensory Nerve Induced Inflammation Contributes to Heterotopic Ossification. J Cell Biochem. 2011 Oct;112 (10):2748-58. PMID:21678472
4. Salisbury EA, ZaWaunyka W. Lazard, Eroboghene Ubogu, Alan R. Davis and Elizabeth A. Olmsted-Davis. Transient Brown Adipocyte-Like Cells Derived from Peripheral Nerve Progenitors in Response to BMP2. Stem Cells Translational Medicine 2012 Dec;1(12):874-85 PMID:23283549
5. Rodenberg E, Lazard ZW, Azhdarinia A, Hall M, Kwon S, Wilganowski N, Merched-Sauvage M, Salisbury EA, Davis AR, Sevick-Muraca EM, and Olmsted-Davis EA. Matrix Metalloproteinase-9 is a Diagnostic Marker of Heterotopic Ossification in a Murine Model. Tissue Eng Part A. 2011 Oct;17(19-20):2487-96. PMID:21599541
6. Lazard ZW, Olmsted-Davis EA, Salisbury EA, Gugala Z, Sonnet C, Davis EL, Beal II E, Ubogu EE, Davis AR. Osteoblasts Have a Neural Origin in Heterotopic Ossification Clin Orthop Relat Res 2015 May 6. (Special Issue on Heterotopic Ossification, guest editor Jonathan Forsberg) PMID 25944403

What opportunities for training and professional development has the project provided? The grant afforded research personnel many opportunities for training. Not only did we manage to be trained by the West Laboratory to bring the PEG-Da hydrogel encapsulation procedures into the Davis laboratory, through mentoring by Dr. West and her group. Additionally mentoring was available to two college students who are interested in careers in science profession and were able to gain, through non-paid volunteer work on the project, beneficial research laboratory experience. Both are determined to enter graduate school upon graduation. Additionally, this work is leading towards several peer-reviewed publications and profession training in presentations of the work at national and local meetings for the students. Also one Post-Doctoral Fellow (Alvarez-Urena) who was paid from institutional fellowship, but focused a component of his time on the project, which resulted in 2 publications for him. See section 6.

How were the results disseminated to communities of interest?
See section 6.

4. IMPACT:

What was the impact on the development of the principal discipline(s) of the project? Completion of the proposed studies significantly advances our knowledge about the essential components of BMP2 induced bone formation. BMP2 as a recombinant protein has been used clinically for many years, but little is known biologically about how it works, and therefore it has never been reliably harnessed for its full potential in bone regeneration and formation. Based on our studies, we have shown a direct role for activation of MMP9 in BMP2 *de novo* bone formation that would be required for spine fusion. This process involves recruitment of neural crest osteoprogenitors from adjacent peripheral nerves, which contribute to robust targeted bone formation. Our studies in mice have shown that this does not appear to damage or lead to any degeneration of the peripheral nerves, because of the organized manner by which the cells exit the nerve. Further for the first time, we have uncovered a potential second factor that is required for BMP2 induced bone formation. Since the data suggests that this involves changes in platelet recruitment that will lead downstream to activation of pro-MMP9 we propose that the second component is TLR3/4 receptor activation. It may not be surprising that this receptor is present on Schwann cells within the endoneurial compartment which is protected by the blood nerve

barrier. Schwann cells express this receptor complex after exposure to our AdBMP2 transduced cells (Data not shown). Therefore, we have filed a disclosure to develop compounds that target this pathway in conjunction with the osteoinductive microspheres to reliably trigger BMP2 induced bone formation regardless of the species. Interestingly, this may explain why several studies have already suggested that the delivery of platelet rich plasma, along with rBMP2 can significantly enhance fracture repair. The data collectively, is a significant advancement to bone tissue engineering and the knowledge about the biological changes that by inclusion of the PEG-Da hydrogel encapsulation of the cells, can rule out immune response to the materials, greatly advances our knowledge about how to translate these types of therapies.

What was the impact on other disciplines? These studies are the first to demonstrate a functional role for active MMP9 in the production of heterotopic bone. This will definitely contribute directly to the development of effective inhibitors for heterotopic ossification, not only in the limb but potentially that associated with vessels and cardiac valves. A large percentage of calcified valves, and some calcified vessels have true bone formation present. Active MMP9 has already been associated with ischemia in the heart, and may be one of the first indicates of early changes that could trigger *de novo* bone formation. The work appears to correlate well already with what is known about changes in vessels during calcific valve disease, therefore, the new findings could further, provide a potential novel treatment options that could be developed and tested in both models. A second discipline that will be impacted by the results is the gene therapy field, where immunity against the vectors has been a huge challenge in developing these types of technologies. The ability to mask the adenovirus from the immune system using PEG-Da hydrogel encapsulation is a huge finding that will aid in advancing this field. Additionally surprising finding is the fact that the mice rapidly raised neutralizing antibodies against adenovirus even when the transduction was done in tissue culture, and no live virus delivered to the mice. Many new strategies in gene therapy are to deliver transduced cells to patients for temporary means of delivering factors. Here we show without the inclusion of the biomaterial these cells will be rapidly irradicated. Finally, the ability for the hydrogel to prevent immunity against the virally transduced cells, and prolong their lifespan in vivo is also a significant advancement in the field of gene therapy.

What was the impact on technology transfer? There where two technologies that were disclosed from this work, and will be important to the translation of this therapy to the clinic. The first is the disclosure of the TLR3/4 modulators that work in conjunction with the BMP2 to evoke reliable bone formation. Secondly, was the finding that active MMP9 appears to be required for the BMP2 induced de novo formation, that does not require structures of bone (periosteum) to be present for bone formation to occur, and that it recruits a neural progenitor in a safe manner to create bone for rapid fusion, or to replace damaged or missing bone. If we can harness this process by inclusion of these modulators we will potentially be able to reliably translate a low dose BMP2 system for spine fusion, and other orthopedic applications.

5. CHANGES/PROBLEMS: See section 1 for discussion of problems. This is a final report so no additional requests are being made.

6. PRODUCTS:

Publications, conference papers, and presentations

- Lu Y, Darned C, Tan I, Zhu B, Hall M, Lazard Z, Davis AR, Simpson S, Sevick-Muraca EM and Olmsted-Davis EA. Far-red fluorescence gene reporter tomography for determination of placement and viability of cell-based gene therapies. Opt Express. 2013 Oct7;21(20):24129-38. PMID 24104323
- Eleanor L. Davis, Corinne Sonnet, ZaWaunyka W. Lazard, Gabrielle Henslee, Zbigniew Gugala, Elizabeth A. Salisbury, Edward V. Striker, Thomas A. Davis, Jonathan A. Forsberg, Alan R. Davis and Elizabeth A. Olmsted-Davis. Location-Dependent Heterotopic Ossification in the Rat Model: The Role of Activated Matrix Metalloproteinase 9. (In Review Journal of Orthopedic Research).
- Alvarez-Urena P, Lazard Z, Sonnet C, Salisbury E, Ramos C, West J, Davis A, **Olmsted-Davis E**. "Cell-based Gene Therapy for Targeted Bone Formation." Military Health System Research

Symposium, 17-20 August 2015, Fort Lauderdale, Florida (poster presentation).

- Davis E.L., Sonnet C., Lazard Z, Salisbury E.A., Nistal R., Davis A.R., and **E.A. Olmsted-Davis**. Location Dependent Heterotopic Ossification in the Rat Model: Absence of Activated Matrix Metalloproteinase 9. 2nd Annual Gulf Coast Consortia Symposium on Regenerative Medicine, June 2015, Houston, TX (poster presentation).
- Davis E.L., Sonnet C., Lazard Z, Salisbury E.A., Nistal R., Davis A.R., and **E.A. Olmsted-Davis**. Location Dependent Heterotopic Ossification in the Rat Model: Absence of Activated Matrix Metalloproteinase 9. Bone Disease Program of Texas, Annual Retreat, May 2015, Houston, TX (poster presentation).
- Sonnet C., Davis, E.L., Salisbury E.A., **Olmsted-Davis E.A**., Lazard Z.W., Beal E, and A.R. Davis. BMP2 Induced *De novo* Bone Formation Utilizes Different Progenitors in Rats Versus Mice and Humans. Center for Cell and Gene Therapy Annual Retreat, Nov 2014, Galveston, TX (poster presentation).
- Sonnet C., Davis, E.L., Salisbury E.A., **Olmsted-Davis E.A**., Lazard Z.W., Beal E, and A.R. Davis. BMP2 Induced *De novo* Bone Formation Utilizes Different Progenitors in Rats Versus Mice and Humans. American Society for Bone and Mineral Research, Annual Meeting, Sept 2014, Houston, TX (poster presentation).
- Olmsted-Davis EA, Davis EL, Sonnet C, Henslee G, Gugala Z, Salisbury EA, Striker EV, Davis AR. Location-Dependent Heterotopic Ossification in the Rat Model: The Role of Activated Matrix Metalloproteinase 9. Bones & Teeth Gordon Conference, Galveston TX, Feb 14-19, 2016 (presentation)
- Pedro Alvarez-Urena, Gabrielle Henslee, ZaWaunyka Lazard, Banghe Zhu, Corinne Sonnet, Carlos Ramos, MD, Jennifer West, Eva Sevick-Muraca, Alan Davis, Elizabeth Olmsted-Davis. (2016). Development of a Cell-based Gene Therapy Approach for Targeted Bone Formation that can be Selectively Turned Off (In preparation for Tissue Engineering).
- Pedro Alvarez-Urena, Gabrielle Henslee, ZaWaunyka Lazard, Corinne Sonnet, Zbigniew Gugala, Jennifer West, Alan Davis, Elizabeth Olmsted-Davis. PEGDa- Hydrogel Encapsulation of Adenovirus Transduced Cells Can Effectively Prevent an Immune Response Against Adenovirus. (2016) (In preparation for Human Gene Therapy)

Inventions, patent applications, and/or licenses

- Patent disclosure: Robust targeted bone formation through delivery of PEGDa hydrogel encapsulated AdBMP2 transduced cells in the presence of activators of the TRL3/4 pathway.
- Patent disclosure: Localized delivery of minocycline for prevention of heterotopic ossification.

7. PARTICIPANTS & OTHER COLLABORATING ORGANIZATIONS

What individuals have worked on the project?

Name:	Elizabeth A. Olmsted-Davis
Project Role:	Principal Investigator
Researcher Identifier (e.g. ORCID ID):	Dr. Elizabeth Davis
Nearest person month worked:	3.6 calendar months/year
Contribution to Project:	Dr. Olmsted-Davis was the PI and oversaw all experiments being done towards the goals of the application. She analyzed all data and was responsible for dissemination through papers and presentations.

Funding Support:	W81XWH-12-1-0475

Name:	Alan R. Davis
Project Role:	Co-Investigator
Researcher Identifier (e.g. ORCID ID):	Dr. Alan Davis
Nearest person month worked:	1.2 calendar months/year
Contribution to Project:	Dr. Davis contributed to the design, analysis, and interpretation of all the data reported in this application
Funding Support:	W81XWH-12-1-0475

Name:	Pedro Alvarez-Urena
Project Role:	Post-Doctoral Fellow
Researcher Identifier (e.g. ORCID ID):	Dr. Alvarez-Urena has left BCM and I know longer have access to his number. He is currently in an entry level faculty position
Nearest person month worked:	6 calendar months/year
Contribution to Project:	Dr. Alvarez-Urena dedicated a portion of his time, conducting the experiments to test the CID through molecular imaging, and also the experiments to look at immune response to the virally transduced cells.
Funding Support:	Other funding source

Name:	ZaWaunyka Lazard
Project Role:	Research Associate
Researcher Identifier (e.g. ORCID ID):	ZaWaunyka Lazard
Nearest person month worked:	6 calendar months/year
Contribution to Project:	She conducted the animal experiments and oversaw purchasing necessary supplies, and handled animal transfers.
Funding Support:	W81XWH-12-1-0475

Name:	Holly Robinson

Project Role:	Research Coordinator
Researcher Identifier (e.g. ORCID ID):	Holly Robinson
Nearest person month worked:	2.4 calendar months/year
Contribution to Project:	She was in charge of all animal handling aspects in the Center for Molecular Imaging. She will coordinate animal transfers between BCM and UTHSC-H and conduct all animal imaging studies.
Funding Support:	W81XWH-12-1-0475

Name:	Nathaniel Wilganowski, M.S.
Project Role:	Research Coordinator II
Researcher Identifier (e.g. ORCID ID):	Nathaniel Wilganowski, M.S.
Nearest person month worked:	2.4 calendar months/year
Contribution to Project:	He analyzed small animal microCT and fluorescence imaging results and compile results for Dr. Sevick to interpret
Funding Support:	W81XWH-12-1-0475

Name:	Eva Sevick-Muraca, Ph.D.
Project Role:	Co-Investigator
Researcher Identifier (e.g. ORCID ID):	Eva Sevick-Muraca, Ph.D.
Nearest person month worked:	0.24 calendar months/year
Contribution to Project:	Dr. Sevick trouble-shooted and interpreted all imaging data obtained during this application
Funding Support:	W81XWH-12-1-0475

Name:	Jennifer West, Ph.D.
Project Role:	Co-Principal Investigator
Researcher Identifier (e.g. ORCID ID):	Jennifer West
Nearest person month worked:	0.24 calendar months/year

Contribution to Project:	Dr. West trouble-shooted and interpreted all data pertaining to the hydrogel encapsulation experiments (Aim 2 and 3).
Funding Support:	W81XWH-12-1-0475

Has there been a change in the active other support of the PD/PI(s) or senior/key personnel since the last reporting period? No

What other organizations were involved as partners?

- Organization Name and Location:

1. Duke University, Durham, NC 27708
    a. Dr. Jennifer West was co-PI and provided a separate budget for her portion of the proposed project. She was instrumental in data collection, troubleshooting all experiments pertaining to the hydrogel biomaterials, and for training additional laboratory personnel on the technologies.
2. University of Texas Health Science Center Houston TX 77030
    a. Dr. Sevick-Muraca was a subcontract on the grant award. She was provided a budget to perform molecular imaging for the Olmsted-Davis laboratory. Dr. Sevick-Muraca provided significant data pertaining on technology to align the bone formation with near infrared imaging, leading to a co-publication. Dr. Sevick's group has also contributed imaging work to a second publication in preparation.

8. COLLABORATIVE AWARDS: For collaborative awards, independent reports are required from BOTH the Initiating PI and the Collaborating/Partnering PI. A duplicative report is acceptable; however, tasks shall be clearly marked with the responsible PI and research site. A report shall be submitted to https://ers.amedd.army.mil for each unique award.

9. APPENDICES: Eleanor L. Davis, Corinne Sonnet, ZaWaunyka W. Lazard, Gabrielle Henslee, Zbigniew Gugala, Elizabeth A. Salisbury, Edward V. Strecker, Thomas A. Davis, Jonathan A. Forsberg, Alan R. Davis and Elizabeth A. Olmsted-Davis. Location-Dependent Heterotopic Ossification in the Rat Model: The Role of Activated Matrix Metalloproteinase 9. (In Review Journal of Orthopedic Research).

Location-Dependent Heterotopic Ossification in the Rat Model: The Role of Activated Matrix Metalloproteinase 9

Eleanor L. Davis[a], Corinne Sonnet[a,e], ZaWaunyka W. Lazard[a], Gabrielle Henslee[a], Zbigniew Gugala[b], Elizabeth A. Salisbury[b], Edward V. Strecker[b] , Thomas A. Davis[f], Jonathan A. Forsberg[f], Alan R. Davis [a,c,d] and Elizabeth A. Olmsted-Davis [a,c,d], *

[a] Center for Cell and Gene Therapy, Baylor College of Medicine, Houston TX 77030

[b] Department of Orthopedic Surgery, University of Texas Medical Branch Galveston TX 77555

[c] Department of Pediatrics, Baylor College of Medicine, Houston TX 77030

[d] Department of Orthopedic Surgery, Baylor College of Medicine, Houston TX 77030

[e] Department of Medicine, Baylor College of Medicine, Houston TX 77030

[f] Regenerative Medicine Department, Naval Medical Research Center, Silver Spring, MD 20910, USA

*Corresponding Author: Elizabeth A. Olmsted- Davis PhD

Baylor College of Medicine

One Baylor Plaza, Alkek N1010

Houston, TX 77030

Email: edavis@bcm.edu

Grant Support: Department of Defense W81XWH-12-1-0274 NIH-NIAMS R21AR063779

Key Words: Heterotopic ossification, BMP2, matrix metalloproteinase-9

ELD, CS, EAS, TAD, JAF, ARD, EAO-D conducted experiments, evaluated the results and drafted the manuscript. ZWL, GH, and EVS conducted experiments and evaluated the results. All authors have read and approved the final version of the submitted manuscript.

Abstract

Extremity amputation or traumatic injury can often lead to the formation of heterotopic ossification (HO). Studies to induce HO in rat muscle using cell-based gene therapy show that this process appears to be location dependent. In the present study, HO was induced in mice and rats through injection of immunologically matched cells transduced with either a replication-defective adenovirus possessing bone morphogenetic protein 2 (BMP2) or an empty adenovirus vector (control). Injection in rat near the skeletal bone resulted in HO, whereas cells injected into the same muscle group but distal from the bone did not result in bone formation. When cells were injected in the same limb at both locations at the same time, HO was formed at both sites. Characterization of the bone formation in rats versus mice demonstrated that different sources of osteogenic progenitors were involved, which may account for the location dependent bone formation observed in the rat. Further experimentation has shown that a potential reason for this difference may be the inability of rat to activate matrix metalloproteinase 9 (MMP9), an essential protease in the mice necessary for recruitment of progenitors. Inhibition of active MMP9 in mice led to a significant decrease in HO. The studies reported here provide insight into the mechanisms and pathways leading to bone formation in different animals and species. It appears that not all animal models are appropriate for testing HO therapies, and our studies also challenge the conventional wisdom that larger animal models are better for testing treatments affecting bone

Introduction

Heterotopic ossification (HO) is formation of bone in soft tissue outside the skeletal bone. HO is induced by traumatic injuries or musculoskeletal diseases, including spinal cord and brain trauma, fractures, muscle contusions, lower motor neuron disorders, genetic disorders, and joint arthroplasty [1] [2] [3].[4] HO may occur proximal to the site of trauma; as seen in amputations. However, HO occasionally forms remotely from the site of injury. Cutaneous burns typically incite HO that is distant from the site of the burn, suggesting that the burn increases osteogenic potential [5] [6].

HO in a rat model can be induced by bone morphogenetic protein 2 (BMP2) [7] [8] or with Achilles tenotomy [9]. Recombinant human bone morphogenetic protein 2 (rhBMP2) is an alternative to autologous bone graft not only because it avoids using a donor, but also blood loss and operative time of a bone graft[10]. Use of rhBMP2 is problematic because it requires large doses of the recombinant protein, well above the endogenous levels of the protein, which can lead to adverse effects. Also use of rhBMP2 requires a foreign carrier and resultant bone formation is highly variable [11]. However, new approaches to deliver rhBMP2 are being tested to limit possible complications [11] [12]. In a rat model described here, cells transduced with a replication-defective adenovirus encoding hBMP2 are injected into the soft tissue to form HO.

The results reveal that the mechanism of HO in the rat is not the same as in the mouse. In the rat, when AdBMP2-transduced cells are injected at a location distal to the skeletal bone, *de novo* bone was not reproducibly formed. For these experiments we define the locations as proximal and distal with respect to skeletal bone, which we define as the origin. Alternatively, when injected proximal to the skeletal bone, HO formed consistently without fusing with the adjacent skeletal bone. Only when the transduced cells were injected both proximal and distal, did bone form consistently at the distal site. Our focus was to discover the mechanistic stages

where the rat and mouse models vary. Our data indicates that although the progenitors in both animal models appear similar, they are recruited from two different locations. Further, a key protein in recruitment of the mouse progenitors, active matrix metalloproteinase 9 (MMP9), was absent in the rats. Interestingly, total MMP9, both active and inactive forms, is found at significantly elevated levels in both species. This finding prompted us to investigate whether active MMP9 is present in soft tissues associated with HO in humans. The data suggests that the activation of MMP9 is changed in the rat model, which could aid in curtailing the formation of ectopic bone.

Materials and Methods

Cell Culture: Primary skin fibroblast cells were from skin biospies from a Wistar rat (WSF) and a C57BL/6 mouse (CSF).

BMP2 Delivery In Vivo: Replication defective E1-E3 deleted first generation human type 5 adenovirus possessing cDNA for BMP2 (AdBMP2) or no transgene (AdEmpty) were constructed as previously described [13]. The control vector lacks a transgene cassette in the E1 region (AdEmpty) [13]. Cells were transduced with AdBMP2 or the Adempty control virus at 7500 vp/cell with 0.75% GeneJammer [14] with transduction efficiency of greater than 90%. Where indicated transduced cells were microencapsulated in poly(ethylene glycol) diacrylate (PEGDA) [15]. In each experiment BMP2 expression was confirmed[13] to be approximately 20 ng/ml /5 x 10^6 cells. Transduced cells were suspended at a concentration of 1 x 10^7 or 5x10^6 cells/100uL of PBS and delivered through intramuscular injection into the hind limb quadriceps of Wistar rats or C57/BL6 mice, respectively. After euthanization, limb tissues were placed either in formalin or snap frozen. All experiments were conducted under an IACUC approved protocol in accordance with OLAW. All animals were housed in an ALAAC accredited vivarium under standard conditions in accordance with OLAW. Animals were randomly selected based on age and health and placed in an experimental group. Each animal was given an experimental number that is

linked only to its group in the medical record. Therefore experimenters involved in data collection and analysis were blinded, and the animal numbers only linked back to groups, for the final data analysis. Group sizes were based on historical power analysis data, however, all power analysis was repeated after data collection to confirm group sizes were adequate.

Minocycline Treatment: Drug was give by intraperitoneal injection 24 hours prior to induction (65mg/kg minocycline in saline or saline alone) and then twice daily with 45 mg/kg. If tissues were harvested to confirm suppression of MMP9, mice received the drug the entire period of the assay, whereas mice where bone formation was quantified received the drug for the first 6 days. Timing was determined by the length of time the cells secreting BMP2 would remain at the location [15] [16].

Tissues Processing: *Paraffin*. Mouse and rat hind limbs were formalin fixed and decalcified before processing. Human tissues were obtained from early heterotopic ossification, from patients undergoing surgeries at Walter Reed Hospital, through an approved IRB protocol. Transfer of tissues to Baylor College of Medicine was done under a separate approved IRB protocol. All human tissue transfers to Baylor College of Medicine (Olmsted-Davis) from Walter Reed (Forsberg) followed the approved Cooperative Research Agreement (CRADA) between BCM and the Department of the Navy. Tissues were shipped in formalin and processed as previously described [17].

Frozen. Skin and skeletal bone were removed from tissues from the rear hind limb of mouse or rat prior to flash freezing. Stained sections were examined by confocal microscopy (Zeiss Inc, Thornwood, NY, LSM 510 META).

Immunohistochemistry: Immunohistochemistry was performed as described [17]. Primary antibodies were used at a dilution of 1:100 to 1:200 and secondary antibodies (Alexa Fluor 488,

594 or 647 (Invitrogen Life Technologies) at a 1:500 dilution. Primary antibodies were as follows: claudin 5 (Novus Biological), CD31 (BD Pharmingen), neurofilament (Sigma-Aldrich), osterix (R & D systems), human mitochondria (Chemicon International), periostin (Abcam), MMP9 (Millipore), MMP9 (Active) clone 4A3 (Millipore).

***Quantification of MMP9 Protein*:** Protein extracts were prepared from muscle (Total Protein Extraction Kit, Millipore, Billerica, MA). Protein concentrations were determined using a Bio-Rad Protein Assay kit® (Bio-Rad Corp, Hercules, CA). Active protein was determined using a MMP9 Biotrak Activity Assay System (GE Healthcare, Piscataway, NJ) and total protein using Quantikine ELISA (R&D Systems). Sample analysis was done in triplicate, and the final values were calculated as the total MMP9 protein within the tissue, as the average of the sample population (n=6), with standard deviation represented with error bars. A paired one-way analysis of variance (ANOVA) with Tukey post hoc correction for multiple comparisons with 95% confidence interval ($p<0.05$) was used for comparisons between days. A student t-test was used to determine significance between treated and control groups.

Microcomputed Tomography: MicroCT of whole hind limb specimens was performed at 7 µm resolution (SkyScan 1174; Micro Photonics Inc, Allentown, PA, USA). A pair of hydroxyapatite phantoms with mineral densities of 0.25 and 0.75 g/cm^3 were scanned alongside each specimen to convert scan data from arbitrary units to units of equivalent bone density. A three-dimensional (3D) region of interest (ROI) was defined for each specimen. Specialized software (CTAn; Micro Photonics Inc, Allentown, PA, USA) was used to analyze microCT images to determine bone volume, mineral density, morphometry, and porosity. Thresholds excluded tissue with a density less than 0.1 g/cm^3, and the tissue volume within ROIs was calculated as a measure of the total bone volume. Tissue mineral content was the total mineral in the region

and tissue density calculated to quantify density of the mineralized tissue. The 3D microCT reconstructions were created using Mimics & Magics software (Materialise; Leuven, Belgium). All quantitative data was analyzed using an ANOVA with Tukey adjustment for multiple comparisons and alpha of 0.05 (SPSS 20; IBM, Armonk, NY, USA).

Results

AdBMP2-transduced cells unable to produce HO in rat.

Previous experiments show mice injected with AdBMP2- transduced cells produce bone within seven days [13]. Similar experiments performed in the rat failed to produce heterotopic bone. This was observed in both wild-type and immune compromised (athymic) rats. Radiological and histological analysis of tissues isolated two weeks after delivery of the Ad5BMP2-transduced cells showed normal muscle tissue with no evidence of HO (Fig. 1B panels c and d, respectively). However, when the injection site was varied (Fig. 1A) within the muscle, results revealed that bone consistently formed when the cells were placed proximal to the skeletal bone (Fig. 1B panels a and b, respectively). The location-dependent HO was consistent even in animals that received a proximal injection of the AdBMP2- cells in one leg (Fig 1C panels a and b) and a distal injection in the opposite limb (Fig. 1C panels c and d). Interestingly, when the cells were injected in the same leg in both a proximal and distal location with respect to the skeletal bone, bone formation was observed at both sites (Fig. 1D panels a-d). To ensure that the cells did not mix, the cells were encapsulated in non-degradable PEGDA hydrogels that allowed the BMP2 to freely diffuse[15]. MicroCT analysis was done on all proximal samples to confirm that the bone was both present as well as distinct from the skeletal bone. Representative microCT images are shown for the animals receiving two injections in the same hind limb (Fig. 1D panel b). In all cases delivery of AdEmpty-transduced cells was used as a control and did not result in bone formation (Fig. 1E).

Addition of stem cells did not rescue the bone formation.

The fact that bone can form in two separate locations in the same limb suggests that the distal site still possesses the ability to respond to BMP2 by forming bone. We hypothesized that the site was capable of making bone but could not expand and recruit necessary progenitors. To test if bone formation could be rescued, AdBMP2-transduced cells encapsulated in PEGDA hydrogel were co-injected with human bone marrow mesenchymal stem cells [18] into the distal location of athymic rats. To ensure that the AdBMP2- cells were capable of inducing HO, they were also injected at a location next to skeletal bone (Fig 2 panel b). However, they were still not capable of inducing bone formation when placed at the distal location (Fig 2 panel a). The MSCs were incapable of rescuing bone formation either when injected with the AdBMP2-transduced cells (Fig 2 panel c) or alone (Fig 2 panel d) since radiological and histological analysis of the tissues two weeks after injection showed no bone formation other than when the BMP2-producing cells were injected at the proximal location. To confirm the stem cell phenotype of the human cells, they were co-injected with AdBMP2-transduced cells into NOD-SCID mice and tracked using an antibody that could selectively detect the human cells. Immunohistochemical analysis showed that after seven days, the cells had incorporated into multiple mesenchymal structures including cartilage and bone (Fig. 2B). The data collectively suggests that these cells were unable to rescue HO.

Osteoprogenitors are similar in rat and mouse, but are derived from different tissues.

We hypothesized that the block in HO formation occurred at the early stages of the process. Therefore, a histological comparison of the tissues was performed. One of the first changes observed in the mouse tissues is the expression of osterix in adjacent peripheral nerves [19] [20]. However, unlike the mouse tissues, rat tissues isolated 1 day after induction showed only a handful of osterix$^+$ cells (Fig. 3A). However, we see an increase in osterix expression over time, with the peak number of osterix$^+$ cells in the nerve seen on day six (Fig.

3A). Additionally, we looked for the expression of the tight-junction molecule claudin 5 that we have previously shown to be present on the nerve-derived osterix^{+} osteoprogenitor in the mouse [20]. Tissues isolated 6 days after induction of bone formation in the rat, surprisingly showed substantial numbers of claudin 5^{+} cells associated with peripheral nerves. Further, a larger number of claudin 5^{+} cells were present than were observed in nerves on the first and second days after induction (Fig. 3A). In the rat, claudin 5^{+} osterix $^{+}$ cells trafficked from the periosteum during bone formation at the proximal location (Fig. 3B). Tissues isolated 2 days after injection of AdBMP2-transduced cells at a proximal site revealed that cells within the fibula appear to be expressing osterix and claudin 5 (Fig. 3B). These cells appear in regions just adjacent to the fibula in tissues isolated on later days (4 and 6 respectively; Fig. 3B.) These cells were also positive for the periosteal marker periostin suggesting they may be derived from this tissue (Fig. 3B). Claudin 5 expression aligned with osterix expression, but not CD31-positive vessels (Fig. 3B), suggesting that they are not a component of local vasculature. The expansion of osteoprogenitors in the rat nerve coupled with their inability to make bone, as well as the observation of migration of osteoprogenitors from the periosteum to the site of bone formation, collectively suggests a block in the ability of osteoprogenitors made in the nerve to exit the nerve during HO.

Active MMP9 is absent in the rat model.

MMP9 has been shown to play a key role in opening the blood-nerve barrier in mouse peripheral nerves during HO [19 20 21], which is a requirement for the entrance of osteoblast progenitors into endoneurial vessels so that they can exit the nerve through the circulation, since endoneurial endothelial cells maintain the tight and adherens junctions comprising this barrier. MMP9 expression and activity has been shown to be significantly elevated in tissues within 24 hours after induction of HO in the mouse model [21]. Surprisingly, MMP9 expression was absent in the rat nerve at similar times, but immunostains to detect the active and precursor

form of the protein (total MMP9) showed positive staining in a number of cells within the reaction site (Fig. 4). To determine if active MMP9 was present, tissues were next immunostained with an antibody that selectively detects only the active form of MMP9. The results showed only a few cells that were positive for the active form at four days after induction of HO with delivery of the AdBMP2 transduced cells (Fig. 4A). Alternatively, the majority of mouse MMP9 was observed to be in the active form, two, four, and six days after BMP2-induction as confirmed by positive immunostaining (Fig. 4B), validating previous conclusions [21]. To determine whether active MMP9 expression was associated with heterotopic ossification in humans, tissues were obtained from patients undergoing active bone formation, and serial sections were immunostained for both the active MMP9 and total MMP9 protein (Fig. 4C). The results show positive staining for both antibodies, and suggest that the majority of the protein is activated in these human tissues.

MMP9 activity was quantified in rat tissues isolated at two, four, and six days after induction of HO. Again, only very low levels of MMP9 activity were detected, with no significant changes between the tissues receiving AdBMP2 -transduced cells and those receiving AdEmpty-transduced cells at 2 and 6 days after induction (Fig. 5A). There was a slight but significant ($p < 0.01$) elevation in MMP9 activity at four days after induction of HO (Fig 5A). MMP9 activity also showed a small but significant increase on day 4 compared to that on days 2 and 6 (Fig. 5A). Previous findings in mice showed that MMP9 activity was significantly elevated on all days (1-6) after induction, confirming the substantial difference between the between rat and mouse [21]. Total MMP9 protein was quantified in these tissues to confirm the presence of proMMP9 in the reaction site (Fig. 5B). Interestingly, total MMP9 was elevated in both rats receiving AdBMP2- and AdEmpty-transduced cells that were isolated 2 days after induction of HO. significant. However, when comparisons of MMP9 total protein levels were made between days, both AdBMP2- and AdEmpty- transduced cells were found to be significantly elevated over the day 6 tissue counterparts ($p < 0.028$ and $p < 0.0086$) suggesting that perhaps the

adenovirus-transduced cells are leading to an inflammatory response and production of the protein. However, total MMP9 levels in the control tissues were significantly reduced by day 4 compared to day 2 ($p< 0.014$), while total MMP9 levels in tissues receiving the AdBMP2-transduced cells remained elevated (no statistically significant difference between day 2) and now was significantly different from the control tissue ($p<0.0056$; Fig 5B). By 6 days after induction of HO, MMP9 protein level was significantly lower in tissues receiving the AdBMP2-transduced cells ($p< 0.025$) as compared to the tissues isolated on day 4, but the control tissues on day 6 were not significantly different those on day 4 (Fig 5B). In contrast, MMP9 total protein expression and activity in the mouse model after induction were significantly elevated during the same time period and remained elevated throughout the course of HO [21]. The data collectively suggests that MMP9 is not activated in the rat, and its expression is quickly down-regulated compared to the mouse.

Suppression of MMP9 significantly reduces HO in mouse.

The data suggests that active MMP9 plays a critical function in the mechanism of heterotopic bone formation. Thus, suppression of MMP9 activation and/or activity in the mouse should prevent heterotopic bone formation. To test this hypothesis mice were treated with the MMP9 inhibitor minocycline or vehicle and resultant heterotopic bone formation assessed by microCT. Results of radiographic analysis show bone formation in all mice; however, there was significantly ($p<0.057$) less total bone formed in the group receiving the MMP9 inhibitor (Fig 6C and D). Immunohistochemical staining for active and total MMP9 protein in tissues isolated 4 days after induction of bone formation showed the presence of MMP9 protein in tissues isolated from both vehicle and minocycline treated mice but a lack of activated protein in tissues derived from mice treated with minocycline, suggesting that it inhibited activation (Fig 6A). The data suggests that MMP9 plays a key role in the process of heterotopic ossification and its lack of

activation in the rat could potentially be responsible for the differences observed between the rat and the mouse.

Discussion

The translation of BMPs into larger animal models has been inconsistent and difficult. Investigators have been unable to see similar effects observed in small animal studies of the BMPs in larger animals such as sheep [22]. The goal of this study was determine why the AdBMP2-transduced cells were unable to produce HO a rat model.

Several differences were noted between HO in the rats versus mice. In the rat, no bone was formed observed when the cells were placed distal to skeletal bone. When the AdBMP2-cells were placed proximal to the skeletal bone, bone formation occurred reliably. Further, when AdBMP2- transduced cells were delivered to both proximal and distal locations, bone formation at the distal site was restored. To ensure that the cell delivery remained at the two locations and did not migrate, we encapsulated them in PEGDA hydrogel microspheres. MicroCT suggests that in both cases the newly forming bone is distinct not only from each other, but also from the skeletal bone. This data suggests that the AdBMP2 -transduced cells do not form HO in rats because they cannot recruit progenitors.

However, addition of mesenchymal stem cells did not rescue bone formation, despite the fact that when these were placed at the site of newly forming heterotopic bone in mice they differentiated into chondrocytes and osteoblasts. This suggests that rescuing the BMP2-induced bone formation in the rat is more complex than delivery of progenitors, and likely involves environmental factors directing progenitor differentiation. These factors appear to be absent in the rat. To identify further differences in the rat that could inhibit bone formation at the distal location, tissues were isolated and examined at early stages of the process. In all cases, we did not observe bone formation in the distal injections, and the delivered cells were rapidly cleared.

Therefore, we focused on the tissues isolated from rats that received the proximal injection and were able to undergo HO.

Immunostaining for osterix and claudin 5, two markers expressed on osteoprogenitors in the mouse showed the presence of cells positive for both markers at the site of new bone formation. In the mouse, the majority of cells within the endoneurium of peripheral nerves adjacent to the site of new bone formation, expressed osterix for 24 hours after delivery of the AdBMP2-transduced cells then disappeared from the nerve prior to the appearance of bone matrix[20]. In the rat, there were only a handful of the osterix$^+$ cells within the endoneurium in the first 24-48 hours after HO induction], but by day 6 there were a substantial number of osterix$^+$ cells in the endoneurium, similar to the amount observed in mouse tissues on day 1[20]. The mouse progenitors were found to be exiting the nerve through endoneurial vessels and circulated to the site of new bone formation (ref). These progenitors could be identified in the circulation as well as in the area of new bone formation by expression of the tight junction molecule claudin 5. In the rat, cells within the endoneurium were negative for claudin 5 until day 6, after which all the cells within the perineurium appeared to be expressing this molecule. The results suggest that the same progenitors as observed in the mouse may be present but in the rat are unable to exit the nerve.

A further surprise was the presence of claudin 5$^+$ osterix$^+$ cells within the periosteum of the fibula in tissues isolated from the rat at 2 days after induction of HO at proximal sites. These cells were also positive for the periosteal marker periostin. On later days (4 and 6) after induction of HO, these osterix$^+$ claudin 5$^+$ periostin$^+$ cells were found surrounding the region where the new bone was forming. Since claudin 5 is also an endothelial cell marker, we next co-immunostained for CD31$^+$ claudin 5$^+$ cells, but at no time were these markers colocalized. The data collectively suggest that claudin 5, the endothelial tight junction molecule found in peripheral nerves, may be expressed on periosteum-derived progenitors in the rat. Further, the

data presented in this report indicate that the rat utilizes similar progenitors, but they are ultimately recruited from a distinct niche.

The term HO refers to *de novo* bone formation in soft tissues but without reference to the distance form skeletal bone. The results presented here are intriguing because the cells delivered proximal to the skeletal bone appeared to generate HO, follow a mechanism similar to a periosteal reaction or orthotopic bone formation through stimulation of the periosteal cells. This raises the question as to whether this is truly heterotopic ossification. Further, the mechanism that prevents periosteal cells from forming new bone contiguous with the skeleton is unclear but warrants future study.

The study results indicate that the recruitment of cells from peripheral nerves in the rat may be problematic. Cells entering or exiting the nerve must pass through the highly regulated blood-nerve barrier, which is controlled by several factors. First, claudin 5^{+} endothelial cells within the endoneurium have been shown to regulate this barrier. However, the barrier is also regulated at the perineurial layer, through claudin 1. Interestingly, one of the only factors known to open this tight junction within the barrier is MMP9 [23]. The opening of the barrier by MMP9 likely occurs through binding and regulation of claudin 1 [23].

Examination of total MMP9 levels in the rat revealed its expression, but not its activation. In experiments where the MMP9 inhibitor minocycline was delivered to mice during the formation of heterotopic bone, the bone formation was significantly decreased with approximately 3-fold less bone volume produced. Bone formation was not completely suppressed in the presence of the MMP9 inhibitor, however, which was a finding similar to previous studies using other inhibitors that affect this pathway [19]. Since the mouse limb is very small, it is difficult to inject the cells distally without having some reside locally near the bone. Potentially the lack of total suppression of bone formation may in part be due to the activation of the periosteum, which is not dependent on this pathway for bone formation. Alternatively, the large amount of active MMP9 found in the soft tissues associated with early HO in human

patients suggests that MMP9 may play a key role in this process. Further, if the partial ablation of HO observed in mice is due to inhibition of the neural pathway without affecting the periosteum, then conceivably targeting MMP9 activation and expression could be more effective in humans, where the entire bone may be of neural origin.

This is the first step in defining the functional role of MMP9 in HO. Understanding the essential role of MMP9 in this process is not only important for developing prophylactic and/or therapeutic interventions against HO, but also may provide new insights to varying efficacies of BMP2 in large animal models. Thus, understanding MMP9's functional role in the process of *de novo* bone formation may provide valuable information to harness the potent HO mechanisms for the regeneration of bone defects and healing fractures.

Figure Legends:

Figure 1: Detection of Heterotopic Ossification (HO). Radiographic and histologic analysis of tissues isolated two weeks after induction of HO. **A.** Representative radiograph showing the location of the distal versus proximal injection sites. **B.** Representative radiographs and photomicrographs of tissues isolated from Wistar rats two weeks after receiving either a proximal or distal injection of AdBMP2 transduced cells. **C.** Representative radiographs and photomicrographs of tissues isolated from a single Wistar rat 2 weeks after receiving a proximal injection of AdBMP2 transduced cells and a distal injection of the same cells in the contralateral limb. **D.** Representative radiograph, microCT image, and photomicrographs of tissue isolated from a single Wistar rat two weeks after receiving a proximal and distal injection in the same limb of microencapsulated AdBMP2 transduced cells. **E.** Representative radiograph, microCT image and photomicrograph of tissue isolated two weeks after injection of Adempty transduced cells.

Figure 2: Human mesenchymal stem cells (hMSCs) were unable to rescue HO.

A. Radiographic and histological analysis of tissues isolated two weeks after induction of HO in the presence and absence of hMSCs. Wistar rats were injected at the distal **(a)** or proximal **(b)** location with AdBMP2 transduced cells and the distal location with hMSCs + AdBMP2 transduced cells **(c)** or hMSCs + PBS **(d).**

B. Photomicrograph of mouse tissue isolated 2 weeks after induction of HO by delivery of AdBMP2 transduced cells in the presence of hMSCs. The differentiation of the hMSCs into mesenchymal tissues of bone was confirmed through immunostaining with an antibody that specifically detects the human cells (brown). The representative section shows the presence of human chondrocytes within the mouse bone.

Figure 3: Representative photomicrographs of immunohistochemical staining of tissues isolated 1, 2, and 6 days after a proximal injection of AdBMP2 transduced cells.

A. Osterix and claudin 5 expression in peripheral nerves within the area of HO. Serial paraffin sections, every 10th slide, were hematoxylin and eosin stained to locate the region of bone formation. Unstained serial sections were then co-immunostained for neurofilament to detect the nerve and the osteogenic factor osterix. Additional sections were also immunostained for claudin 5 an osteogenic marker in mice.

B: Osterix and claudin 5 expression in the periosteum of the fibula near site of HO. Serial paraffin sections, every 10th slide, were hematoxylin and eosin stained to locate the region of bone formation. Unstained serial sections were then immunostained for osterix (osteoprogenitors). Serial sections were also co-immunostainned with claudin 5 and CD31 to determine if the cells expressing claudin 5 were associated with the vasculature and periostin to confirm that the cells were associated with the periosteum.

Figure 4: Expression of MMP9 active and inactive forms within the area of HO. Representative photomicrographs of paraffin sections serially cut from rat (**A**), mouse (**B**), or human (**C**) tissues. Rat and mouse tissues were isolated 2, 4 and 6 days after delivery of AdBMP2 transduced cells. Human tissues depict soft tissues immediately surrounding the newly

forming heterotopic bone. Tissue sections were stained with hematoxylin and eosin or co-immunostained with antibodies that detect total MMP9 (red) or the active form (green), or for human tissues total MMP9 (green) and active form (red) as indicated.

Figure 5: Quantification of MMP9 protein and functional activity by ELISA. Tissues were isolated from rats at 2, 4, and 6 days after proximal injection of AdBMP2 and AdEmpty transduced cells and protein extracts generated. (**A**) MMP9 protein was bound through ELISA, and then substrate added, to quantify MMP9 functional activity. (**B**) MMP9 total protein was bound through ELISA and quantified directly. Standard amounts of active MMP9 or total MMP9 protein respectively were assayed in order to calculate active protein amount from the activity measurements. Statistical significance was calculated using a standard t-test, with n=6.* denotes statistical significance. Sample comparisons between the various days were calculated using a paired one-way ANOVA with Tukey post-hoc correction for multiple comparisons with 95% confidence interval ($p<0.05$). A student t-test was used to determine significance between the treated and control groups.

Figure 6: Quantification of HO in mice treated with minocycline or vehicle. Mice were treated with minocycline or vehicle and HO induced through delivery of AdBMP2 transduced cells. (**A**) Tissues isolated at 4 days were immunostained for the presence of both total MMP9 (green color) and active MMP9 (red color) expression. (**C and D**) Bone formation was quantified in tissues isolated 14 days after induction of HO and three dimensional reconstruction of the resultant bone is depicted. (**E**) Bone volume was then calculated from each animal (n=4) and the average volume and standard error of the mean depicted. Statistical significance was determined by student t-test with confidence interval of 95% ($p<0.05$). * denotes statistical significance.

1. Baird EO, Kang QK. 2009. Prophylaxis of heterotopic ossification - an updated review. J Orthop Surg Res 4:12.
2. Alfieri KA, Forsberg JA, Potter BK. 2012. Blast injuries and heterotopic ossification. Bone Joint Res 1:192-197.
3. Salisbury E, Sonnet C, Heggeness M, et al. 2010. Heterotopic ossification has some nerve. Crit Rev Eukaryot Gene Expr 20:313-324.
4. Zotz TG, Paula JB, Moser AD. 2012. Experimental model of heterotopic ossification in Wistar rats. Braz J Med Biol Res 45:497-501.
5. Ipaktchi K, Mattar A, Niederbichler AD, et al. 2006. Attenuating burn wound inflammatory signaling reduces systemic inflammation and acute lung injury. J Immunol 177:8065-8071.
6. Wu X, Rathbone CR. 2013. Satellite cell functional alterations following cutaneous burn in rats include an increase in their osteogenic potential. J Surg Res 184:e9-16.
7. Shi S, de Gorter DJ, Hoogaars WM, et al. 2013. Overactive bone morphogenetic protein signaling in heterotopic ossification and Duchenne muscular dystrophy. Cell Mol Life Sci 70:407-423.
8. Wang M, Abbah SA, Hu T, et al. 2013. Minimizing the severity of rhBMP-2-induced inflammation and heterotopic ossification with a polyelectrolyte carrier incorporating heparin on microbead templates. Spine (Phila Pa 1976) 38:1452-1458.
9. O'Brien EJ, Frank CB, Shrive NG, et al. 2012. Heterotopic mineralization (ossification or calcification) in tendinopathy or following surgical tendon trauma. Int J Exp Pathol 93:319-331.
10. Campana V, Milano G, Pagano E, et al. 2014. Bone substitutes in orthopaedic surgery: from basic science to clinical practice. J Mater Sci Mater Med 25:2445-2461.
11. Wang M, Abbah SA, Hu T, et al. 2015. Polyelectrolyte Complex Carrier Enhances Therapeutic Efficiency and Safety Profile of BMP-2 in Porcine Lumbar Interbody Fusion Model. Spine (Phila Pa 1976).
12. Olabisi RM, Lazard Z, Heggeness MH, et al. 2011. An injectable method for noninvasive spine fusion. Spine J 11:545-556.
13. Olmsted-Davis EA, Gugala Z, Gannon FH, et al. 2002. Use of a chimeric adenovirus vector enhances BMP2 production and bone formation. Hum Gene Ther 13:1337-1347.
14. Fouletier-Dilling CM, Bosch P, Davis AR, et al. 2005. Novel compound enables high-level adenovirus transduction in the absence of an adenovirus-specific receptor. Hum Gene Ther 16:1287-1297.
15. Olabisi RM, Lazard ZW, Franco CL, et al. 2010. Hydrogel microsphere encapsulation of a cell-based gene therapy system increases cell survival of injected cells, transgene expression, and bone volume in a model of heterotopic ossification. Tissue Eng Part A 16:3727-3736.
16. Fouletier-Dilling CM, Gannon FH, Olmsted-Davis EA, et al. 2007. Efficient and rapid osteoinduction in an immune-competent host. Hum Gene Ther 18:733-745.
17. Olmsted-Davis E, Gannon FH, Ozen M, et al. 2007. Hypoxic adipocytes pattern early heterotopic bone formation. Am J Pathol 170:620-632.
18. Ramos CA, Asgari Z, Liu E, et al. 2010. An inducible caspase 9 suicide gene to improve the safety of mesenchymal stromal cell therapies. Stem Cells 28:1107-1115.

19. Salisbury E, Rodenberg E, Sonnet C, et al. 2011. Sensory nerve induced inflammation contributes to heterotopic ossification. J Cell Biochem 112:2748-2758.
20. Lazard ZW, Olmsted-Davis EA, Salisbury EA, et al. 2015. Osteoblasts Have a Neural Origin in Heterotopic Ossification. Clin Orthop Relat Res 473:2790-2806.
21. Rodenberg E, Azhdarinia A, Lazard ZW, et al. 2011. Matrix metalloproteinase-9 is a diagnostic marker of heterotopic ossification in a murine model. Tissue Eng Part A 17:2487-2496.
22. Egermann M, Lill CA, Griesbeck K, et al. 2006. Effect of BMP-2 gene transfer on bone healing in sheep. Gene Ther 13:1290-1299.
23. Hackel D, Krug SM, Sauer RS, et al. 2012. Transient opening of the perineurial barrier for analgesic drug delivery. Proc Natl Acad Sci U S A 109:E2018-2027.

Figure1:

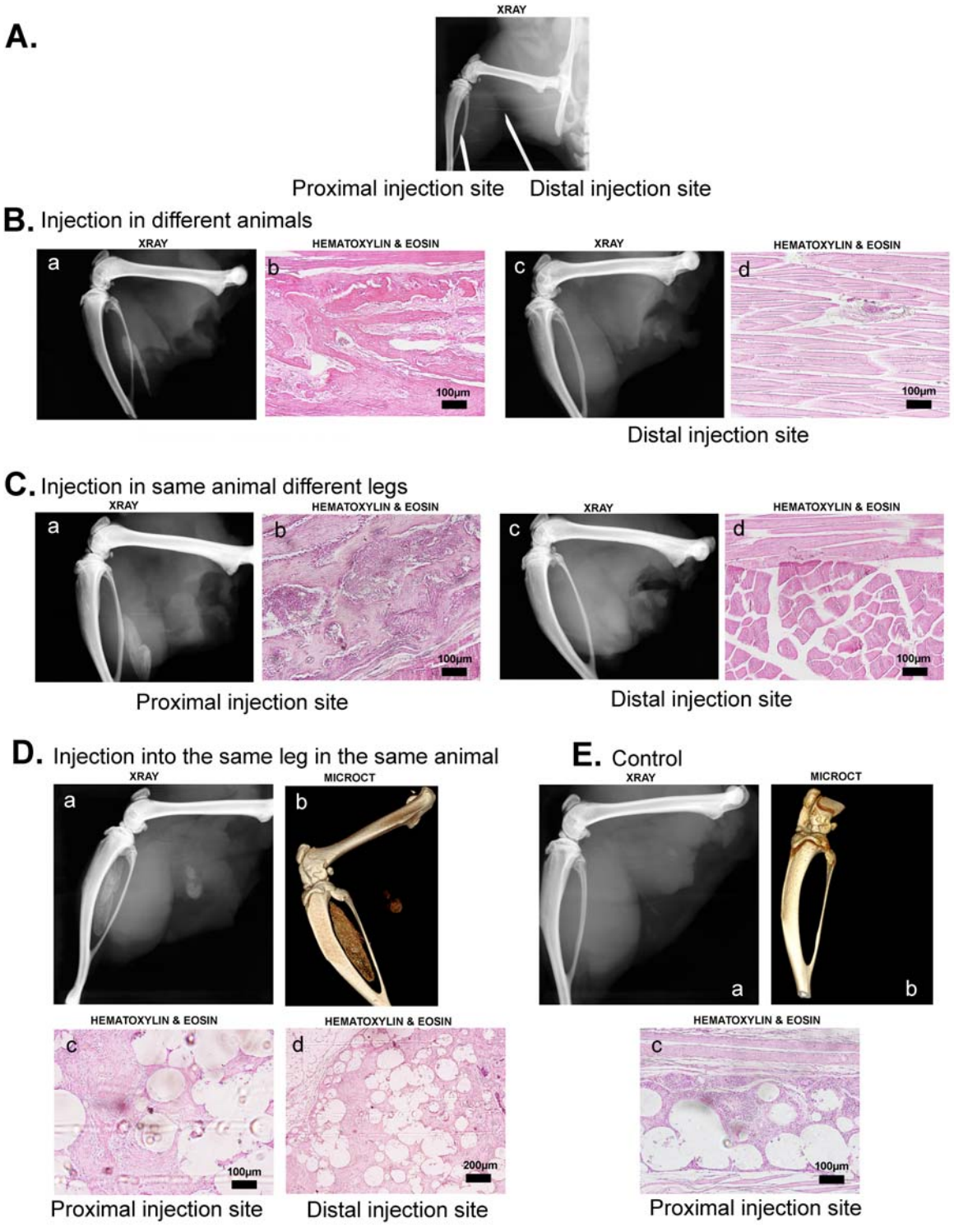
A.
XRAY
Proximal injection site
Distal injection site
B. Injection in different animals
XRAY
HEMATOXYLIN & EOSIN
a
b
100µm
XRAY
HEMATOXYLIN & EOSIN
c
d
100µm
Distal injection site
C. Injection in same animal different legs
XRAY
HEMATOXYLIN & EOSIN
a
b
100µm
XRAY
HEMATOXYLIN & EOSIN
c
d
100µm
Proximal injection site
Distal injection site
D. Injection into the same leg in the same animal
XRAY
MICROCT
a
b
HEMATOXYLIN & EOSIN
HEMATOXYLIN & EOSIN
c
d
100µm
200µm
Proximal injection site
Distal injection site
E. Control
XRAY
MICROCT
a
b
HEMATOXYLIN & EOSIN
c
100µm
Proximal injection site

Figure 2:

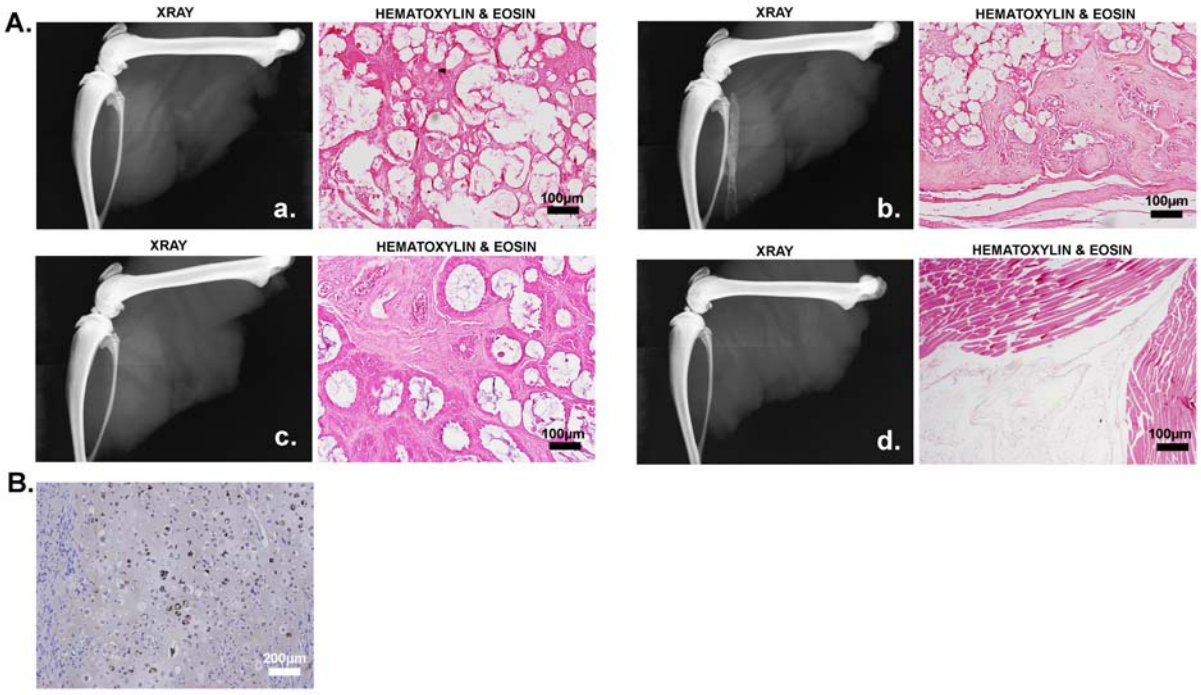
A.
XRAY
HEMATOXYLIN & EOSIN
a.
100µm
XRAY
HEMATOXYLIN & EOSIN
b.
100µm
XRAY
HEMATOXYLIN & EOSIN
c.
100µm
XRAY
HEMATOXYLIN & EOSIN
d.
100µm
B.
200µm

Figure 3:

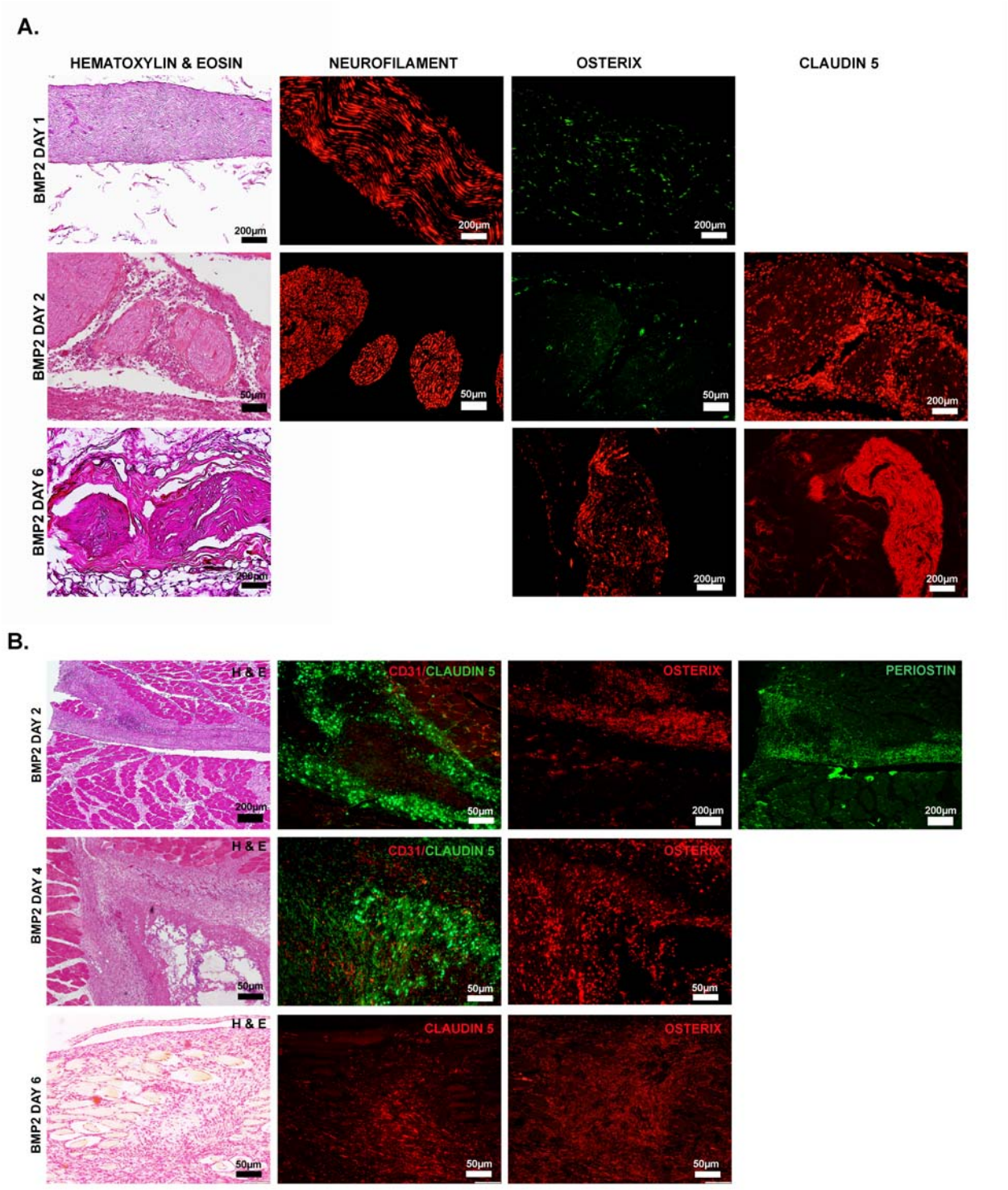
A.
HEMATOXYLIN & EOSIN
NEUROFILAMENT
OSTERIX
CLAUDIN 5
BMP2 DAY 1
BMP2 DAY 2
BMP2 DAY 6
200μm
50μm
B.
BMP2 DAY 2
BMP2 DAY 4
BMP2 DAY 6
H & E
CD31/CLAUDIN 5
OSTERIX
PERIOSTIN
CLAUDIN 5

Figure 4:

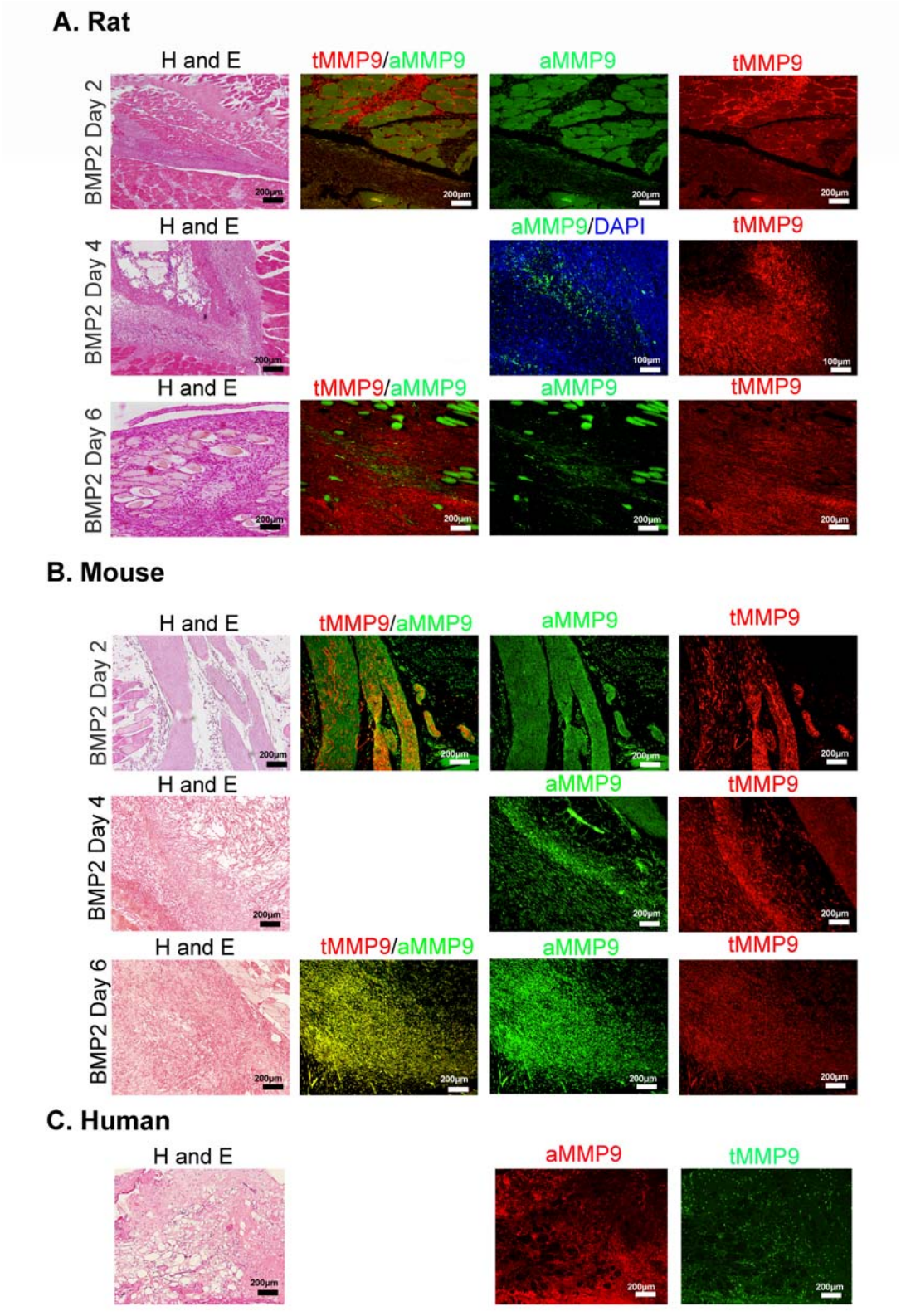
A. Rat
H and E
tMMP9/aMMP9
aMMP9
tMMP9
BMP2 Day 2
H and E
aMMP9/DAPI
tMMP9
BMP2 Day 4
H and E
tMMP9/aMMP9
aMMP9
tMMP9
BMP2 Day 6
B. Mouse
H and E
tMMP9/aMMP9
aMMP9
tMMP9
BMP2 Day 2
H and E
aMMP9
tMMP9
BMP2 Day 4
H and E
tMMP9/aMMP9
aMMP9
tMMP9
BMP2 Day 6
C. Human
H and E
aMMP9
tMMP9
200μm
100μm

Figure 5A:

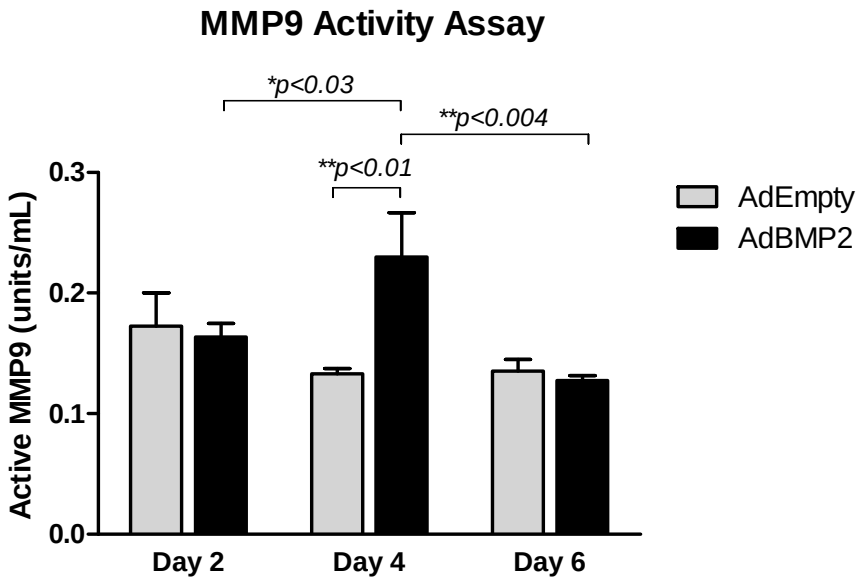
MMP9 Activity Assay
*p<0.03
**p<0.004
**p<0.01
Active MMP9 (units/mL)
0.3
0.2
0.1
0.0
Day 2
Day 4
Day 6
AdEmpty
AdBMP2

Figure 5B

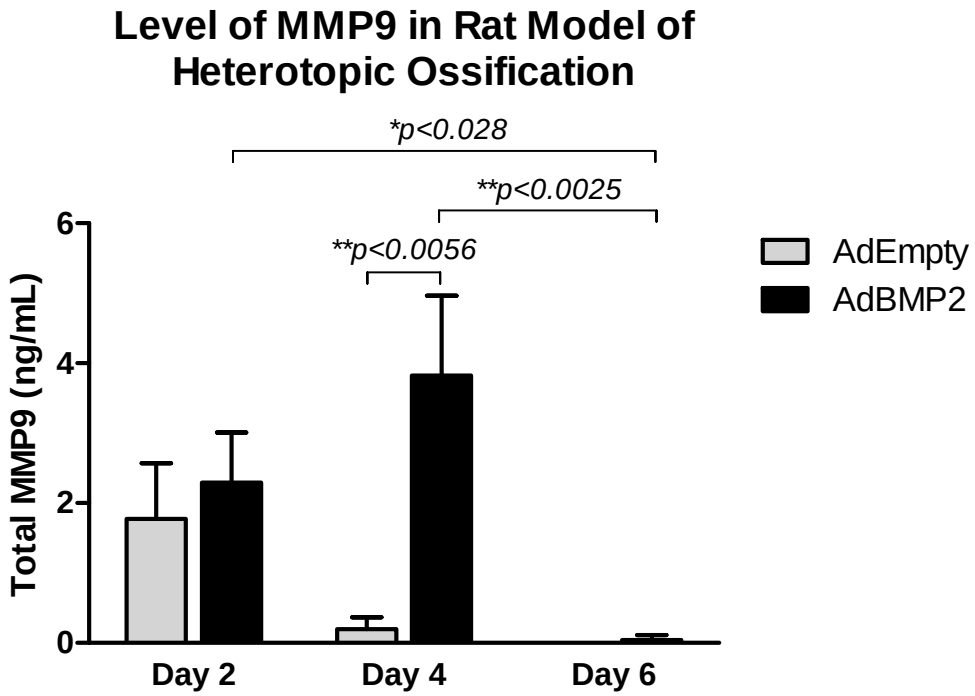
Level of MMP9 in Rat Model of Heterotopic Ossification
*p<0.028
**p<0.0025
**p<0.0056
Total MMP9 (ng/mL)
6
4
2
0
Day 2
Day 4
Day 6
AdEmpty
AdBMP2

Figure 6:

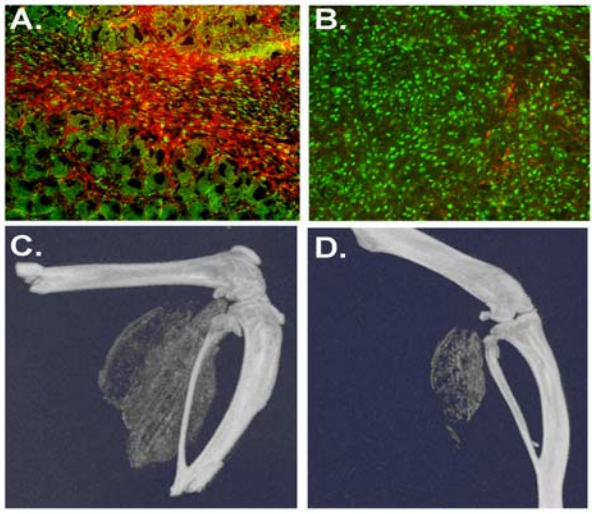
A.
B.
C.
D.

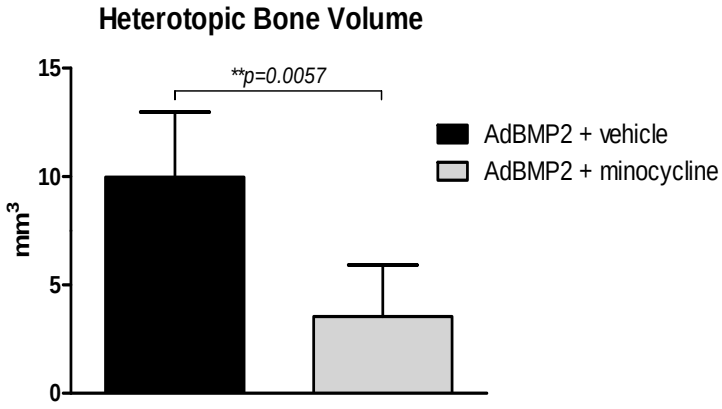
Heterotopic Bone Volume
**p=0.0057
15
10
5
0
mm3
AdBMP2 + vehicle
AdBMP2 + minocycline